PROCESSING SPEED IN AGING BRAIN: A FUNCTIONAL MRI STUDY USING SIMPLE STIMULUS-RESPONSE MAPPING TASK

HO YIN WONG

PhD

The Hong Kong Polytechnic University

2019

The Hong Kong Polytechnic University

Department of Rehabilitation Sciences

PROCESSING SPEED IN AGING BRAIN: A FUNCTIONAL MRI STUDY USING SIMPLE STIMULUS-RESPONSE MAPPING TASK

Ho Yin WONG

A thesis submitted in partial fulfilment of the requirements
for the degree of Doctor of Philosophy

August 2018

CERTIFICATE OF ORIGINALITY

I hereby declare that this thesis is my own work and that, to the best of my knowledge and belief, it reproduces no material previously published or written, nor material that has been accepted for the award of any other degree or diploma, except where due acknowledgement has been made in the text.

______________________________(Signed)

__________Ho Yin WONG__________(Name of Student)

Abstract

Processing speed mediates cognitive declines due to aging. However, the neurophysiological mechanisms that compromise processing speed remain understudied. In addition, the processing-speed paradigms employed in existing studies may be confounded by sensory, motor, and executive functions, especially among old participants.

In this study, a set of simple stimulus-response mapping tasks in two perceptual modalities were used to establish the contribution of functional activation and connectivities on processing speed in young and old participants; the aim was to minimize the influences of the sensory, motor, and executive functions. This study further divided processing speed into decision and non-decision components to characterize the contributions of the neurophysiological properties. The most significant set of predictors were then identified in both the young and older groups to facilitate comparisons between those groups.

The final sample included 34 young (aged 18-28) and 20 old (aged 65-75) healthy adults. This study employed visual and audial forms of a stimulus-response mapping task at two levels of difficulty and with a simple response-time task to control for the sensorimotor-related processes. The processing time index (PTI), sensorimotor time index (STI) and cognitive time index (CTI) were statistically derived from reaction-time (RT) measures. Common regions of interests (ROIs) were identified for all the experimental conditions using anatomically defined brain parcellations. Estimated time series for these brain activations were then extracted, as were the effective connectivities. Multivariate structural autoregression was applied to all time series and all ROI (separately for each subject and for each task condition).

Bootstrapped mixed-effect lasso (least absolute shrinkage and selection operator) regressions were employed to select the local activations and the interregional effective connectivities so as to predict the values of the three speed indices.

For both groups, the bilateral regions of the medial frontal cortex (MFC), anterior insula, superior frontal junction (SFJ), intraparietal sulcus, and cerebellum were activated in all mapping tasks; 13 total ROIs were selected. In the younger group, three local activation predictors and seven effective connectivities were associated with at least one of the three speed indices. Nearly all of these were associated with the right superior MFC and the cerebellum vermis VI and VII; only one causal influence was associated with the right SFJ and the left intraparietal sulcus, as reflected by decision speed (CTI). In the older group, seven activation predictors and five connectivity predictors were associated with speed indices. The predictors associated with the bilateral SFJ and bilateral intraparietal sulcus were unique to the older group.

The younger participants' processing speed was supported by the regions related to the MFC (which was implicated in sustained cognitive control), the vermis (which was presumably the automatic counterpart of different frontal functions), and the connection from the left SFJ to the left anterior intraparietal sulcus (which facilitated stimulus-response mapping). The MFC and vermis were also strong predictors of processing speed in the older group. However, the association in the vermis VI/VII/VIII demonstrated incompatible pattern, reflecting a cerebellar adaptive function in the older group. In addition, a more diverse network involving the SFJ and the intraparietal sulcus was also associated with the speed indices, suggesting that the older group engaged the attention function more than the younger group did.

PUBLICATIONS ARISING FROM THE THESIS

Poster

Wong, C. H. Y. (2016). The Role of Default Mode Network in Mediating Processing Speed Function (p. 38). Presented at the 22nd Annual Meeting of the Organization for Human Brain Mapping, Geneva, Switzerland.

Journal

Wong. C. H. Y., Liu J., Tao J., Lee T. M. C., Wong A. W. K. Chau B. K. H., Chen L., Chan C. C. H. Medial Frontal Cortex and Cerebellar Vermis Mediating Cognitive Processing Speed using Attentional Task. In preparation.

ACKNOLEDGEMENTS

First and foremost, I would like to express my gratitude to my chief supervisor, Professor Chetwyn Chan, for his patience, guidance, encouragement and support throughout my PhD study over the years.

I am thankful to have Dr. Vincy Cheung as my co-supervisor who encouraged me to pursue the academic career.

I would also like to thank the staff and laboratory members in the Applied Cognitive Neuroscience Laboratory. I have learned a lot from them in the lab meetings.

Special thanks to the staff in Fujian University of Traditional Chinese Medicine and all the participants in this study.

Most of all, I would like to thank my wife, Edith and my son, Daniel. They gave me love and support to complete the PhD study.

I thank God who always gives me new challenges. Ebenezer.

TABLE OF CONTENT

LIST OF TABLES

LIST OF FIGURES

Chapter 1 Introduction

Cognitive decline has been associated with aging. A wealth of literature supports the idea that processing speed mediates the age-related decrement of cognitive constructs such as working memory, executive control, and complex cognition (Albinet, Boucard, Bouquet, & Audiffren, 2012; Schretlen et al., 2000; Verhaeghen, 2011). Despite the importance of processing speed in cognition, the neurophysiological mechanisms that determine the speed of information processing have not yet been well-established. Although neuroimaging researchers have examined the roles of regional and global deficits in gray and white matter, only a few have used functional imaging to evaluate the contributions of regional brain activations and the cross-talk among various neural substrates. Another issue with the current literature is the absence of examinations of the cerebellum. This gap is mainly due to the long history of associations between the cerebellum and motor control, as the most prominent theories have been built around the frontal and parietal lobes. However, researchers have recently shown the cerebellum's role in cognition; in particular, the results of a large-scale volumetric study (Eckert, 2011) revealed the importance of the cerebellum in determining processing speed. The goals of this dissertation are threefold: dividing processing speed into cognitive- and sensorimotor-related components, establishing neurophysiological and neuroanatomical correlates, and focusing on the fronto-parieto-cerebellar network's role in processing speed.

The sensorimotor and cognitive components of processing speed were thus separated. The majority of recent functional imaging studies of processing speed have utilized single measures (mainly visual paradigms). To this end, a two-by-two experimental design was adopted to minimize bias with regard to sensory modality and task demand, and the neural correlates were modeled using a multivariate approach. Using this approach, the common associations among neurological and behavioral measures were maximized across the various task demands.

The literature review (Chapter 2) contains a review of the research on processing speed as a psychological construct, including the neuroimaging studies on processing speed and the related experimental findings. Methodological and statistical considerations are also described in that chapter. Chapter 3 details the study's research paradigm, as well as its data preprocessing and statistical analysis methods. The behavioral results for the young and older groups are reported in Chapter 4. Chapter 5 reports the imaging results for the task-related activations and the selection of the ROIs. 0 focuses on the predictors of activations and connectivities for the speed indices in the normal young adults and includes a discussion of the mechanisms that facilitate speedy processing in the younger participants. Chapter 7 contains the same results for the older participants and a discussion of the reasons for this group's deficits and its possible compensatory mechanisms. Chapter 8 concludes the thesis, explicates the study's limitations, and outlines future research directions.

Chapter 2 Literature Review

Chapter Summary

This chapter is divided into five sections. The first section introduces the theoretical foundations of processing speed in the context of cognitive aging. The second section contains a discussion of the methodological considerations, with a focus on the decision to use the behavioral paradigm and on the study's aim. The third section is intended to explain the neurological foundations of processing speed. The fourth section provides a review of the statistical methods that are relevant to the investigation of this thesis's research questions. The chapter ends with a list of hypotheses that address those research questions.

Definitions of Processing Speed and the Related Research Traditions

Processing speed is the speed of completing a task or process; it involves responding to a stimulus according to certain rules. There are two schools of thought in studies of processing speed (Jensen, 2006). The first takes an experimental perspective and employs various components of response time to make inferences regarding a hypothetical situation or a series of neural processes (Posner, 2005). The studies in this school of thought commonly involve systematic manipulations of a stimulus's perceptual quality or the rules that govern the response outputs that a participant generates. The time involved in completing certain processes can be inferred from the differences in the response times. The second school of thought regards processing speed as a psychological construct that characterizes individual or group differences (McAuley & White, 2011; e.g. Nielsen & Wilms, 2014). Researchers have tended to rely on batteries of tests to examine processing speed (R.

D. Roberts & Stankov, 1999). The common latent factors that explain the results of these tests inform the construct of the processing speed. The relationships between these common latent factors and other psychological constructs (such as working memory, executive function, and long-term memory; Verhaeghen, 2011) or other external variables (such as gender, age, and clinical conditions) are explored through multivariate statistics such as structural equation modeling (e.g. Schmiedek, Oberauer, Wilhelm, Süß, & Wittmann, 2007). The current thesis is focused on exploring the potential differences in the neural mechanisms that underlie processing speed among both young and old participants. In particular, the focus is on understanding age-related variability so as to enrich the knowledge gathered by both schools of thought in this field.

Reasons to Study Individual Differences in Processing Speed

In everyday life, people have to make quick responses in a wide variety of scenarios. Answering the phone when it rings, pressing the open-door button in an elevator, and keeping up with responses when engaging in a group game all require timely and spontaneous actions. Members of some occupations, such as bus drivers, athletes, and firefighters, require the ability to make quick responses as part of their day-to-day work. The Cattell–Horn–Carroll theory of human intelligence considers processing speed to be a broad ability that contributes to general intelligence (Carroll, 1993; Schneider & McGrew, 2012). Processing speed is a predictor of academic achievement among students (Mulder, Pitchford, & Marlow, 2010; Rohde & Thompson, 2007). Slow processing speed is associated with various clinical conditions, including schizophrenia (Barch & Ceaser, 2012), attention deficit hyperactivity disorder (S. L. Calhoun & Mayes, 2005), traumatic brain injury (Hillary et al., 2010), and multiple sclerosis (Costa, Genova, DeLuca, & Chiaravalloti, 2016). In one of the most prominent theoretical accounts of the impact of slowness in cognitive performance, (Salthouse, 1996; 2000) asserted that delays early processes limit the time that is available for later processes, which can lead to the decay of early processes before the later parallel processes are complete. The slowing of cognitive processes can thus impact a wide array of cognitive functions.

In the course of life-span development, processing speed appears to follow an inverted-U-shaped trajectory (Kail & Salthouse, 1994; Verhaeghen, 2013a). Processing speed improves in childhood and adolescence before peaking in early adulthood (Hale, 1990) and declining through middle and old age (Verhaeghen, 2013a). Furthermore, processing speed has been shown to be a precursor of other cognitive abilities. In adolescence (Coyle, Pillow, Snyder, & Kochunov, 2011) and old age (Finkel & Pedersen, 2010; Verhaeghen, 2011), processing speed has been proposed as a mediator of the development and decline across age groups of cognitive abilities such as working memory (Chiaravalloti, Christodoulou, Demaree, & DeLuca, 2003), episodic memory (T. Lee et al., 2012), executive control (Verhaeghen, 2011), divergent thinking (Preckel, Wermer, & Spinath, 2011), and fluid intelligence (Schretlen et al., 2000; Wilhelm & Oberauer, 2006)—but not crystallized cognition (Verhaeghen, 2013a). Processing speed is also correlated with intelligence (Deary, 2001; Der & Deary, 2003) and has been regarded as the key indicator of cognitive aging (Finkel, Reynolds, McArdle, & Pedersen, 2007).

It is important to understand the neural basis underlying individual differences in cognitive aging. From an individual perspective, maintaining cognitive youthfulness is important to quality of life in late life. Because cognitive aging is associated with activities of daily living (Han, Gill, Jones, & Allore, 2016), it is beneficial to identify the factors that could slow down such a decline, including the maintenance of cognitive (Bielak, Hughes, Small, & Dixon, 2007), social (Fratiglioni, Paillard-Borg, & Winblad, 2004), and physical (Rikli & Edwards, 1991) activity. From a societal perspective, average life expectancy has increased by 10 years in the past two decades (Murray et al., 2015), and poor cognitive aging has burdened both caregivers and community services (Han et al., 2016). It is worth mentioning that processing speed is also associated with the daily functioning of older adults, both with and without mild cognitive impairments (Bezdicek, Stepankova, Martinec Novakova, & Kopecek, 2016; Owsley, Sloane, McGwin, & Ball, 2002; Perneczky et al., 2006).

Common Measures of Processing Speed

Two types of instruments are involved in the operationalization of processing-speed measures. The first type is psychometric tests, which are predominantly paper-and-pen measures, such as the digit-symbol substitution task, symbol-search task, and cancellation task in the Wechsler Adult Intelligence Scale (Wechsler, 2008). In these tests, the participants receive a list of items (printed on paper) and must write their responses within a fixed amount of time. The number of accurately completed items is then converted into a score for the processing-speed test. The tasks in such tests are designed to be simple, with the assumption that the majority of the subjects will complete the entire task if given enough time to process all the items. The neural processes involved in this type of task commonly include visual search and the comparison of visual symbols. The most popular processing-speed measure in both functional neuroimaging studies (Baudouin, Clarys, Vanneste, & Isingrini, 2009; Genova, Hillary, Wylie, Rypma, & DeLuca, 2009; Habeck et al., 2015; Rypma et al., 2006; Salthouse et al., 2015) and structural MRI studies (Costa et al., 2016; Gazes et al., 2016; Miller et al., 2013; Nazeri et al., 2015; Turken et al., 2008) is the digit-symbol substitution task. In the paper-and-pen version, this task includes a coding table that contains two rows and nine columns. The cells in the top row contain single-digit numbers from 1 to 9, and those in the bottom row contain corresponding abstract symbols for each digit. The subject completes the test by examining each number in a separate table and writing the corresponding symbol for those numbers within a fixed duration. The number of accurate answers is considered that person's processing speed.

Another type of task that is used in measuring processing speed is a custom-designed protocol, which involves presenting a stimulus and simultaneously recording the participant's response and reaction time (RT, on a millisecond scale). The classic test is the one used in Donder's (1969) seminal study of RT; another example is a modern computerize measures of elementary cognitive tasks (ECT; Jensen, 2006). In this type of measure, the subject receives instructions that define the rules for responding to the stimulus. The stimuli are then presented on a computer screen or through a speaker, and the subject's responses are recorded with an input device such as a keypad, keyboard, or joystick. The subject's RTs (the time between the stimulus onset and the recorded response) and accuracy are recorded for each of a given number of trials. Summary statistics are calculated for all trials, using the same conditions for each individual so as to facilitate group comparisons.

In functional imaging settings (e.g. Rypma et al., 2006), the digit-symbol substitution task has been adapted to include a response pad inside a scanner. Because of this, the digit-symbol substitution task has been split into discrete trials. For each trial, the subject is shown a coding table in the top half of the screen and a digit-symbol pair in the lower half of the screen. The digit-symbol pair could be an exact match for one of the pairs in the table, or the symbol could correspond to a different number. The subject responds to indicate if the stimulus is a match. Hence, this task involves a two-choice response. The accuracy rate and the mean response time can then be used for further statistical comparisons. In this way, the computerized digit-symbol substitution task is a version of ECT. Hence, the boundary between psychometric tests and ECTs appears to be blurred among neuroimaging studies.

Neurological Bases of Processing Speed

A few questions remain unanswered in the context of aging effects on processing speed. Why are processing-speed measures sensitive to cognitive aging? What is the cause of this slowdown in the elementary processes?

To address those questions, this thesis is divided into two studies. The first study is based on young adults' results for the core components of processing speed using functional MRI. The young adults were chosen because the trajectory of the change in processing speed across the life span peaks in this age group. The neural substrates for which their activations contributed the most to the speed of information processing were identified by modeling the associations between the neurophysiological and speed measures. At the time of this writing, only a few researchers had explicitly studied the neurophysiological correlates of processing efficiency in normal young adults (Forn, Ripollés, et al., 2013a; Forn, Rocca, et al., 2013b; Rypma et al., 2006)—sometimes as a control reference for clinical groups (Akbar et al., 2016; Genova et al., 2009; Leavitt, Wylie, Genova, Chiaravalloti, & DeLuca, 2012; Woodward, Duffy, & Karbasforoushan, 2013)—or for the aging population (Motes, Biswal, & Rypma, 2011). These studies employed modified digit-symbol tests or visuospatial tasks such as visual searches and pattern comparisons

(Carlozzi, Beaumont, Tulsky, & Gershon, 2015; Salthouse, 2000). However, the results of previous behavioral studies challenged the idea that the digit-symbol test taps into not only processing speed but also executive control (Cepeda, Blackwell, & Munakata, 2013). The nonspecificity of the digit-symbol test with regard to processing speed is further aggravated among the older-adult population (Albinet et al., 2012). This challenge is corroborated by the activations of the dorsolateral prefrontal cortex (DLPFC; (Rypma et al., 2006), and the causal influence that the left DLPFC has on the ventral frontal and posterior brain (Biswal, Eldreth, Motes, & Rypma, 2010) is associated with RTs on the digit-symbol test. These findings lend support for the use of experimental tasks involving simple (rather than complex) cognitive processes in the studies in this thesis.

A review of the functional brain-imaging studies on processing speed indicates that the majority have been based on visual-based paradigms. For instance, the digit-symbol test, letter comparisons, and pattern comparisons involve visual search and the encoding of visual stimuli (Forn et al., 2009; Genova et al., 2009; Habeck et al., 2015; Rypma et al., 2006). In summary, the measured speed-related activity in those existing studies is biased toward the visual modality of processing and uses a limited set of mental operations. The first study in this thesis, therefore, was aimed at revealing the basic elements of processing speed by designing two simple and comparable cognitive tasks, as well as a control response task, using visual or audial stimuli. These simple cognitive tasks were anticipated to provide more control over other cognitive processes (apart from processing speed) as well as over the confounding variables, as they use of a single modality (visual or audial stimuli). The second study in this thesis employed the same experimental tasks—a simple cognitive process and two stimulus modalities—to explore aging's effects on processing speed. The differences between the young and the older groups could illuminate how age-related cognitive decline (and perhaps compensatory mechanisms) modulate processing speed among the older participants.

Rypma (2006) conducted the first study on processing speed, using the digit-symbol task and a functional imaging method; the same paradigm was later used in studies of processing speed among patients with multiple sclerosis (Akbar et al., 2016; Genova et al., 2009) and among older adults (Motes et al., 2011). A recent initiative on the Reference Ability Neural Network (RANN), researchers have incorporated the digit-symbol task with two other cognitive tasks to study the processing-speed construct (Habeck et al., 2015; 2016) with an event-related design. In each trial, a coding table and a digit-symbol pair were shown to the participants, who then used a response pad to indicate whether that test pair matched one of the nine digit-symbol pairs in the table. Not all researchers had participants respond by hand; others have adopted a form of the digit-symbol task that requires participants to respond orally (Forn et al., 2009; 2011; Forn, Ripollés, et al., 2013a; Forn, Rocca, et al., 2013b). In these studies, instead of a probing pair, the participant viewed a coding table and one of the abstract symbols from that table; the participant would then read the number corresponding to that symbol in the table. Another characteristic of these studies was the use of a block design with a short inter-trial interval (less than 2 s); the number of accurate trials was the indicator of processing speed. The results revealed that processing speed was associated with activations in the bilateral DLPFC, the ventral lateral prefrontal cortex (PFC), the SFJ (also referred to as the frontal eye field), the bilateral intraparietal sulcus, the superior MFC, and the occipital lobe.

Back to the RANN series of studies (Habeck et al., 2015; 2016), the activations associated with the participants' responses in a set of 12 cognitive tasks informed the latent factors of four reference abilities: processing speed, episodic memory, fluid reasoning, and vocabulary. The common neural substrates showed activations associated with the RTs across all 12 cognitive tasks in the left postcentral gyrus, left inferior parietal gyrus, bilateral dorsal striatum (including the caudate and putamen), bilateral visual cortex, and left precentral gyrus (Habeck et al., 2016). Habeck et al. (2016) attributed these neural substrates' activation patterns to visuomotor function (left postcentral gyrus and left inferior parietal gyrus), motor coordination (dorsal striatum), visual input (occipital), and motor output (precentral gyrus). Habeck and colleagues also found that all the tasks shared a common activation-and-deactivation network that resembled the task-positive network (Fox et al., 2005) and the default node network (Raichle & Snyder, 2007). The task-positive network is similar to those that have been reported in other studies of the digit-symbol paradigm (Forn, Rocca, et al., 2013b). The topography of the all these networks, including the ability-specific and ability-common networks, are invariant across the life span. For specific networks derived from the younger group (aged 20-30), the results were nonsignificant when tested on older groups (people in their 30s, 40s, 50s, 60s, and 70s). The participants of different age groups tended to recruit nondifferentiable neural substrates to mediate the processing speeds of each of the domain-specific tasks. Habeck et al. (2016) also used machine-learning techniques on functional MRI data (which was collected for the 12 tasks in the four domains) to verify the similarities. They trained the classifier to learn the activation patterns of the four reference domains and then tested the classifier with an independent set of data. Interestingly, they found that classification accuracy was associated with behavioral performance in the other three reference-ability domains, but not in the speed domain. These findings suggest that speed performance is not particularly associated with speed-related substrates and is instead more associated with the common network identified in the study: the task-positive network (Fox et al., 2005).

Scholars who have reported speed-related neural correlates have further supported the argument that the common task-positive network is associated with processing speed. Neural networks seem to provide more meaningful interpretations than isolated neural substrates for task-related RTs. Among young adults, lower activations in the dorsal PFC and higher activations in the ventral PFC, as well as in the occipital and parietal regions, are all associated with shorter RTs on the digit-symbol test (Rypma et al., 2006). Rypma et al. (2006) then conducted a Granger causality analysis on eight ROIs, including the dorsal PFC (BA9), posterior PFC (BA46), ventral PFC (BA44), and parietal cortex (BA40). Subjects with shorter RTs showed less interregional causal influence and fewer frontal-to-parietal connections. Rypma et al. suggested that higher activations in the ventral PFC and in the parietal and occipital cortices indicated efficient visual search processes and hence, lower frontal control requirements. Higher activations in the dorsal PFC reflected increased executive control and executive monitoring among those whose RTs were relatively slow. In contrast, the slow participants showed higher frontal activations and greater influence on posterior regions. More reciprocal frontal-to-parietal causal influences, according to Rypma et al., were related to the control and monitoring functions. Therefore, the speed-related activations were apparently driven by the control and processing modules within the task-positive network. The higher activations observed in the ventral PFC and parietal cortex among those who had faster RTs may have reflected a higher degree of automatic processing during the tasks (Rypma et al., 2006).

However, as Rypma and colleagues (2009) noted in a later review, different task manipulations may have influenced the performance-related activations. Forn, Ripollés, and colleagues (2013a) reported on the task-load manipulation of an oral-response version of the digit-symbol task in which they manipulated the load by varying the frequency of the stimulus (using inter-trial intervals of 1.5, 2 and 2.5 s). Forn, Ripollés, and colleagues found that the activations of the medial superior frontal cortex and intraparietal sulcus increased with the task load; they also found that the frontoparietal control network (Cole, Repovs, & Anticevic, 2014b) and the two cerebellum networks (identified using independent component analysis) were also recruited at the highest load. Importantly, they reported two performance-related activities only at the highest load (inter-trial intervals of 1.5 s). The activation of the MFC (involving the pre-supplementary motor area and the anterior cingulate cortex) and the task-relatedness (degree of engagement) of the frontoparietal control network were both negatively associated with the percentage of correct answers, indicating that efficient subjects required less activation of the MFC and less interregional connectivity. Although the latter finding (less interregional connectivity for fast subjects) was consistent with Rypma and colleagues' (2006) results, the former (less performance-related activation) was not. The discrepancy may be related to the task manipulations.

In Rypma's (2006) implementation, the participants had to encode both the symbol and the digit in working memory, but in Forn, Ripollés, and colleagues' (2013a) implementation, the participants only had to encode the symbol, and the oral response was more intuitive than in Rypma's (2006) implementation. The implementation in (Forn, Ripollés, et al., 2013a) adaptation involved scanning (the symbol) and reading (the digit), but that in Rypma's (2006) adaptation required scanning (the digit), matching (the symbol), response selection (match or not match), and a motor response (left or right). The differences in working-memory load and stages of processing explained the significant performance-related activations that were found in the DLPFC in Rypma's (2006) study—but not in Forn, Rocca, and colleagues' (2013b) study; these activations were attributed to cognitive control. On the other hand, performance-related activation occurred in the medial prefrontal cortex (Forn, Rocca, et al., 2013b) in the condition with the highest speed demands. According to (Forn, Rocca, et al., 2013b), medial prefrontal cortex was "implicated in finding relevant stimuli, being ready for action, feedback monitoring and response-related processing, and is reinforced by activation of the anterior cingulate gyrus as a central structure of alertness and vigilance, which is activated during response selection mechanisms" (p. 158), and the pre-supplementary motor area was implicated in making response with time pressure (Forstmann et al., 2008). Because Rypma (2006) adapted an event-related design, the inter-trial interval ranged from 4 to 12 s; the lack of speed-related activation in was due to the small interval. Given that the original design of the paper-and-pen version of the digit-symbol test was constrained by time, the accelerated version that (Forn, Rocca, et al., 2013b) used was similar to the original.

Motes and colleagues (Motes et al., 2011) explored the aging effect using the same paradigm that Rypma et al. (2006) used. They reported significant age-by-performance interactions in the bilateral dorsal PFC (anterior middle frontal gyrus, BA9 and 10), right SFJ (frontal eye field, BA6) as well as in the left temporal pole and cerebellum; younger participants demonstrated negative performance-activation correlations (lower activations for faster participants), and older participants demonstrated positive performance-activation correlations (higher activations for faster participants). Motes and colleagues (2011) suggested that the negative performance-activation correlations in the PFC for the younger group indicated that these younger participants, who were more efficient, relied less on the control or coordination of the subprocesses of the PFC; this would be related to a higher degree of process automation among the younger participants. In the older group, Motes and colleagues interpreted the positive performance-activation correlations in the PFC as a consequence of that group having both less availability of prefrontal resources and degraded automaticity. There were also significant group differences in the task-related activations. Older participants demonstrated stronger activation in the bilateral motor cortex (which may have been due to compensatory recruitment) and weaker activation in the visual cortex and right parahippocampus (which may have been due to functional loss). The roles of the left temporal pole and cerebellum in mediating the positive performance-activation correlations in the left lateral PFC (BA46) and occipital lobe in both groups remains unexplained, however.

In a structural MRI study, Eckert et al. (2010) reported a neural network consisting of the DLPFC, the MFC, and a cerebellar component; this network was related to processing speed. Eckert and colleagues (2010) studied the structural correlates of processing speed in 42 adults (aged 19-79), using source-based morphometry to analyze the spatial volumetric covariations across the regional volumetric density, so as to study the age-related volumetric correlation of processing speed. Eckert and colleagues revealed seven neural components; of these, both the DLPFC and MFC component and the cerebellar component demonstrated age-related structural correlates, as measured with the Connect Simple Test (Salthouse, 2000). These findings fit with those of the previously reviewed functional imaging studies. Several studies of aging participants (e.g. Miller et al., 2013; Nadkarni et al., 2014) and those with multiple sclerosis (e.g. Moroso et al., 2017; Ruet et al., 2014) have also indicated cognitive slowing with reduced cerebellar volume.

The results of the studies reviewed above suggest that the efficiency of information processing during the digit-symbol task can be explained by at least two constructs: the cognitive-control mechanism (supported by activations of the anterior middle frontal gyrus or BA9, and of the pre-supplementary motor area or anterior cingulate cortex, as well as the connectivity of the frontoparietal control network) and the automaticity of processes (supported by the activation of the ventral PFC and of the parietal and occipital lobes). These results suggest that the digit-symbol task may be overly complex (Albinet et al., 2012; Cepeda et al., 2013) if the primary goal of the study is to measure processing speed, as the RTs of the responses in the task are likely to include the times taken for both executive control (such as sequencing subprograms) and actual execution. The frontoparietal network, which mediates the executive control, relates to programming (or breaking) a task into subprocesses and to supervising the timing of those subprocesses (see Dosenbach et al., 2007; Duncan, 2010). In a meta-analysis of 119 studies, (Verhaeghen, 2011) concluded that processing speed explains a great amount of the variance in executive function, and associated that speed with cognitive declines due to aging. As suggested in factor-analysis studies (Danthiir, Wilhelm, Schulze, & Roberts, 2005; R. D. Roberts & Stankov, 1999; Stankov & Roberts, 1997), simple speed measures (ECTs) and complex psychometric measures share a common variance. Putting this information together, the most common psychometric tests involve a considerable amount of executive control (Albinet et al., 2012; Cepeda et al., 2013), such that, in the meta-analysis (Verhaeghen, 2011), processing speed was shown to mediate the relationship between aging and executive control. The results reviewed above further support the choice of simple ECT instead of psychometric tasks for studies of processing speed in old populations.

Another suggested component of processing speed is stable task-control processes, which are mediated by the medial frontal cortex (MFC) (Dosenbach et al., 2006). Speed-activation correlations of the medial PFC reveal that task-control processes involve sustained attention, feedback monitoring, and response selection (Forn, Rocca, et al., 2013b). A further postulate is that these task-control processes sustain across trials within an entire block (Dosenbach et al., 2006). Fan (2014) used information-processing theory to explain that activations of the MFC demonstrate that speed is influenced by the amount of the information that the MFC processes in a fixed time unit, which is a bottleneck in task performance. This interpretation is corroborated by the observation that significant activations of the MFC are coupled only with the task blocks that are contained in a high number of trials (Forn, Rocca, et al., 2013b).

The third candidate for the processing-speed component is the top-down attention-orientation system, as subserved by the dorsal attention network (Corbetta & Shulman, 2002). This network consists of the bilateral SFJ (or frontal eye field), and the bilateral intraparietal sulcus—a main portion of the task-positive network (Fox et al., 2005). Scholars have reported intra-network coactivation in studies of macaques (Vincent et al., 2007) and humans (Fox & Greicius, 2010) in a resting state; they have also observed task-induced activation and functional connectivity in broad categories of experimental paradigms (Cole, Bassett, Power, Braver, & Petersen, 2014a; Hugdahl, Raichle, Mitra, & Specht, 2015), including processing-speed paradigms (Forn, Ripollés, et al., 2013a; Habeck et al., 2016). In particular, Motes and colleagues' (2011) observed activations in the right frontal eye field, thus demonstrating an age × speed interaction effect. Motes and colleagues also reported positive performance-activation correlations in the older group but negative correlations in the younger group. These results have been interpreted as the engagement of a compensation mechanism. I propose that the differences in the correlations are due to two mechanisms. First, in the younger group, the task is completed before the attention system becomes fully engaged, so the degree of activation is positively associated with on-task time. Second, in the older group, faster subjects engage the attention system to a greater degree so as to compensate for the loss of function in other brain areas, so higher activation is associated with greater effort and shorter processing time.

An unexplained but consistent finding relates to the cerebellum's contribution to processing speed. Activation (Motes et al., 2011); the task-relatedness of cerebellar-related networks (Forn, Ripollés, et al., 2013a) and their structural correlates (Eckert et al., 2010) with processing speed have been reported. In particular, Hogan (2004), in the fronto-cerebellar aging hypothesis, suggested that control (automaticity) accounts for the cerebro-cerebellar interaction. Hogan also suggested that the cerebellum integrates sensory, motor, and cognitive information through feedforward and feedback mechanisms, with feedforward-feedback oscillation cycles creating a synchronization effect, and with the variability (or instability) disrupting the processing efficiency. This also provides a biological mechanism for the oscillation theory of cognitive slowing (Jensen, 2006). Shine and Shine (J. M. Shine & Shine, 2014) provided an account along the same lines, suggesting that cognitive control could be made automatic through the delegation of control from the cortex to the cerebellum.

The involvement of cerebellum in stimulus-response mapping tasks has been evidenced using functional imaging. First, Balsters et al, (2012) using different stimulus-response rules, found differentiable level of rule-specific activations, which suggested that the activation of cerebellar is modulated by the complexity of rule, but not exclusively motor coordination. Second, Brissenden et al. (2018) used the whole brain MVPA (multi-voxel pattern analysis) method to study the rule-specific brain activation pattern, and they found that cerebellum encoded the stimulus-response mapping rules. Third, by analyzing the activation pattern of visual working memory and attention task with different level of cognitive load, Pischedda et al (2017) found a dorsomedial-to-ventrolateral activation gradient in the cerebellar, and they also reported a similar gradient in the intraparietal sulcus, suggesting that the cerebellum hold a parallel representation as that in the parietal lobule. The authors interpreted that the cerebellar contained an internal model for similar cognitive processes as in the cortex. In general, recent imaging studies supported the cerebellum supported the stimulus-to-response mapping.

In summary, processing speed probably has four components: moment-to-moment adaptive control (supported by the DLPFC and lateral frontal-parietal network), stable task-set control (supported by the MFC), top-down attention orientation (supported by the SFJ and intraparietal sulcus), and automaticity (supported by the cerebellum).

Summary of Neurophysiological Speed-correlate

Previous fMRI study of processing speed reported several factors contributed to better performance in the younger group, including lower activation of the dorsolateral prefrontal cortex, the medial frontal cortex and right frontal eye-field, less causal influence from dorsolateral prefrontal cortex and less dorsal attention network task-related coactivation, and higher activation of task-related processes in the posterior parietal and cerebellum. The findings were attributed to less top-down cognitive control, less top-down attention control and more automaticity of task-specific processes. In the old group, higher activation of dorsolateral prefrontal cortex and right frontal eye-field were associated with better performance, which was ascribed to compensatory mechanism of the prefrontal cortex.

Reaction Time Measures

For RT-based measures, mean and median RT are the most popular ways to obtain scores for an individual; some studies have also utilized the standard deviation of RTs to explore intra-subject variability in task performance. As the RT distribution is usually positively skewed, some researchers fit RTs to various distribution models so as to estimate and to describe the non-Gaussian properties of the distribution. Ex-Gaussian (Dawson, 1988), ex-Wald (Schwarz, 2001), gamma (Dolan, van der Maas, & Molenaar, 2002), and Weibull (Logan, 1992) distributions have been popular in behavioral studies of RTs (Palmer, Horowitz, Torralba, & Wolfe, 2011). Most researchers have derived mathematical models to mimic the negative Gaussian tail and the positive exponential tail of the RT distribution using a few parameters, while fitting the RT data for the correct trials to the model and estimating the parameters for each individual. However, there is no consensus about the interpretation of the parameters. For example, there are differing opinions regarding whether the exponential tail of the ex-Gaussian distribution is free from the decision component (Palmer et al., 2011).

(Ratcliff, 1978) diffusion model has received the most attention of any model in the field, and researchers have used that model to separate the decision component from the perceptual component so as to identify the association between white-matter integrity and decision speed. However, this method was not applicable to the current study, as several subjects achieved 100% accuracy in the experimental tasks, and as the diffusion model requires the RTs of the inaccurate trials to infer the speed of information accumulation.

Mass-Univariate Analysis, Multiple Regression and Variable Selection

To make a prediction regarding behavior based on a neuroimaging data set, the neuroimaging community must overcome the problem of data with a large *p* (many predictors) and a small *n* (small sample size), as the number of observations (voxels) is far larger than the number of subjects in these data sets. Mass-univariate analysis has been the most popular method since the introduction of the SPM package in 1999. The standard procedure for whole-brain correlational analysis involves normalizing an individual statistical map to a template space, fitting a linear model to each voxel, and statistically correcting for multiple comparisons (Ashburner & Friston, 2000). However, there are several drawbacks to this method.

First, the mass-univariate analysis relies on Gaussian random field theory to conduct cluster-based, family-wise corrections that control for type I errors. Gaussian random field theory is based on the smoothness of the data, the cluster size, and the clusters' significance values. The drawbacks of this theory include its arbitrary clustering parameters, its collapse of spatially connected but functionally orthogonal regions into one cluster, and its favoring of large clusters over smaller ones.

Second, the relative contributions of various neural substrates in behavioral measures can only be inferred qualitatively—by comparing the significance levels of the behavioral correlates. In recent years, scholars have adapted several statistical techniques in imaging studies.

Third, a variable's contribution could be suppressed by other variables, causing the simple correlation to fail to detect the association between the brain marker and the behavioral measure (R. L. Smith, Ager, & Williams, 1992). In particular, creating a response to a stimulus involves a train of cognitive processes, such as sensory registration, recognition, attention orientation, binding a rule to a mental representation, action selection, and motor execution; these processes contribute to the RT. Assuming that RT is just a linear combination of processing time of those components, the process that takes longest time could mask the effect of the processes that take less time. To this end, multiple regression is used in this study instead of mass-univariate analysis.

However, the problem of having a large p and small n cannot be resolved. In particular, there are more than 200,000 voxels in the Montreal Neurological Institute (MNI) template, and even when the whole brain is parcellated using the Desikan atlas (Desikan et al., 2006), there are still 34 cortical regions, which could cause overfitting and thus hamper the generalizability of the selected model (McNeish, 2015). A popular approach is to use stepwise regression to select the predictors that have the most predictive power; however, the collinearity of the predictors is a known problem for stepwise regression. The efficiency of the processing modules could be affected by a common factor, such as the integrity of white matter (e.g. Nazeri et al., 2015) or genes (e.g. Laukka et al., 2015), such that the processes' performances are not orthogonal. To this end, this study used lasso regression (Tibshirani, 1996; 2011) to explore the contribution of neurophysiological factors. Lasso regression deals with both variable selection and regularization, and it provides a sparse solution to improve the model's interpretability (McNeish, 2015). Regularization, specifically, involves adding a penalizing term to the cost function of the ordinary least square such that the magnitudes of the coefficient estimates shrink. Modifying the weight (λ) of the penalizing term causes the coefficients of the less relevant variables to shrink to zero. In this study, the best model was chosen by searching for the λ that would minimize prediction errors through cross-validation. Statistically, a sparse model is one that contains a small number of predictors. Ridge regression (Hoerl & Kennard, 2012), another regularized regression technique, assigns a coefficient for every predictor, so it is not sparse. Researchers have recently advocated for the use of such a technique in studies of the genome (e.g. T. T. Wu, Chen, Hastie, Sobel, & Lange, 2009) and those that use imaging (Abram et al., 2016; Bunea et al., 2011), as sparse models outperform other regression methods in searches for biomarkers. To further improve model selection, the current study included bootstrapping for the lasso regression (Bunea et al., 2011; Laurin, Boomsma, & Lubke, 2016), as this method has been shown to improve models by removing predictors that have small effects.

The Knowledge Gap

As illustrated above, there are a few gaps in the existing literature on processing speed. First, few researchers have directly explored individual differences in processing speed using functional MRI. Second, the majority of the existing literature on individual differences in processing speed relates to the digit-symbol task, in which the task processes are likely to be contaminated by executive functions (specifically, the demand for adaptive control). This contamination is more serious if the participants choose to employ individualized strategies when searching, matching, and responding during the task. Third, the speed measure is likely to be dominated by the use of visual stimuli. The visual processing involved in the task would bias the speed-activation associations in such functional brain imaging studies. Fourth, the role of the cerebellum and the cerebro-cerebellar interactions in processing speed are underresearched.

Aim

This thesis revisits the mechanisms that underlie processing speed with tasks that involve a low level of executive control. The experimental tasks used in this study were based on a two-choice RT paradigm that is sensitive enough to measure speed. The design of the task also incorporated better control of the sensory, motor, and task-specific processes. To control for sensory registration and motor response, as Jensen (1990) suggested, the control condition was a simple RT task. To control for the task-taking processes, the contrast condition was another two-choice RT task (with a lower level of difficulty). To reduce the bias toward a single perceptual modality, each of three task conditions had visual and audial versions of perceptual modalities. The task content was modified from the arrow task (T. M. C. Lee et al., 2006; 2005)—a visual stimulus-response choice RT task—and converted into three task conditions (control, 1-rule, and 2-rule), each with two modality versions (visual and audial).

In this study, the various components were embedded in the behavioral RTs through the use of a CTI that was derived by subtracting the sensorimotor time (simple RT) from the processing time (stimulus-response mapping RT, Figure 2-1) by means of lasso regression. The concept and the method behind the CTI computation are covered in the method section of this thesis.

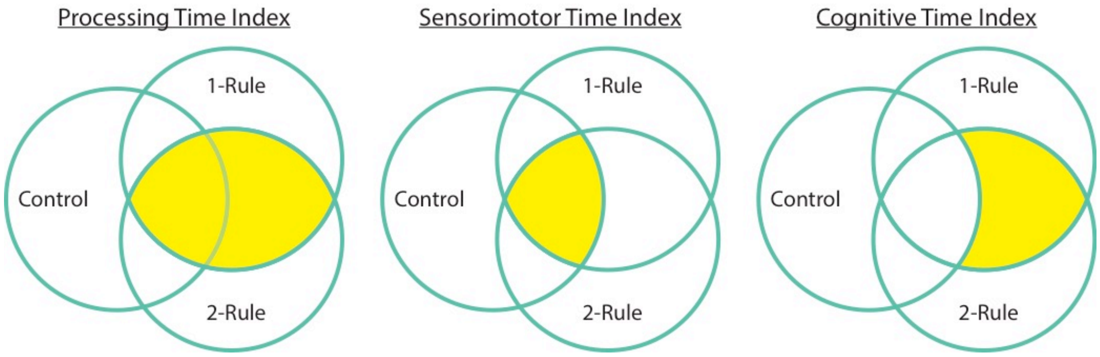

Figure 2-1 Conceptual illustration of operationalization of behavioral indices

Hypotheses

The hypotheses in this study are as follows:

1. In the younger group, faster processing speed is associated with relatively low activations in the frontal lobe and relatively high activations in the parietal lobe and the cerebellum.
2. In the younger group, faster processing speed is associated with less causal influence.
3. In the older group, faster processing speed is associated with more frontal activations.
4. For the older group, as compared to the younger group, faster processing speed is associated with more activations due to the causal influence of the frontal-to-parietal and frontal-to-cerebellar interactions.

Chapter 3 Method

Participants

Forty healthy young adults aged 18-28 and forty healthy old adults aged 65-75 participated in the study. The final sample contained 34 young (21.5±2.1 years, 14 females) and 20 old (66.8±2.7 years, 12 females) adults as six young and twenty old participants were excluded due to premature response more than 40% of trials in any condition (<150ms, 1 young) or missing more than 40% of the trials in any condition (2 young, 18 old), or below 70% accuracy in any condition (4 young, 2 old). All participants had normal vision and audition, were right-handed as screen by the Edinburgh handedness questionnaire (Oldfield, 1971), and had high school education or higher. They were recruited from the local communities close to the Fujian University of Traditional Chinese Medicine where the study was conducted. The exclusion criteria were: cognitive impairment (Montreal Cognitive Assessment, Beijing Version (Yu, Li, and Huang 2012), MoCA<26), depressive mood (Hamilton Rating Scale for Depression, Frank et al. 1991, HAMD>=7), neurological diagnosis which could affect cognitive functions (such as brain injury and post-stroke), substance abuse/smoking, sub-normal audio-visual function or MRI scan contraindications. E Standard Logarithm Eyesight Table was used to ensure the subjects have normal or correct-normal vision. For the audition, we use the pure-tone detection to test the hearing abilities of subjects. Pure-tone detection thresholds at octave frequencies ranging from 300 to 1000 Hz were within normal limits in both ear (Collignon et al. 2011, Böhr et al. 2007). All participants were explained the purpose of the study. Their informed consent was obtained prior to the training and experimental procedures. Ethics approval was obtained from the Ethics Committee of the Fujian University of Traditional Chinese Medicine.

Experimental Tasks

The Arrow task (T. M. C. Lee et al., 2005; 2006) was modified into three task conditions: two two-choice reaction time tasks with different task-taking rules, and a simple reaction task as the control (Figure 3-1). The two-choice tasks involved participants to encode and discriminate the visual or audial stimuli, and give motor responses according to the rule set out in the task. The 1-rule condition was to press the “UP” button upon viewing an “upward” arrow (for visual stimuli) or upon listening to a “high-pitch” tone (for audial stimuli); or press the “DOWN” button upon viewing a “downward” arrow or listening to a “low-pitch” tone (Figure 3-1). The 2-rule condition was to give responses which are the reverse of those in the 1-rule condition, i.e. “UP” button for a “downward” arrow or a “low-pitch” tone, or “DOWN” button for an “upward” arrow or a “high-pitch” tone. The control condition was to press any button upon viewing a vertical line without an arrow head (or listening to a “mid-pitch tone”). It was anticipated that a control trial would involve vigilance and focused attention, and motor response processes. The 1-rule trial would involve discrimination and response selection, in addition to those for the control trial. The 2-rule trial would further require binding of the stimulus-response mapping rule (seeing “upward” arrow for pressing “DOWN” button), of which the original 1-rule representation itself (seeing “upward” arrow for pressing “UP” button) contained the response rule (Wilhelm & Oberauer, 2006).

The design of visual and audial stimuli in each of the three task conditions was to tackle the potential confounds of modality commonly committed in previous studies on processing speed. The task trials were presented using a block design. The visual and audial versions of the tasks were organized in two separate runs. For each run, there were 15 task blocks. Each block had 10 of 1-rule, 2-rule or control trials. The 15 task blocks were randomized and counter-balanced in each run. The total number of trials in each condition was 50. Preceding each block, the subject was reminded about the button-press response by showing the instruction on the screen for four seconds. For each trial, the stimulus was presented for 800 ms, followed by a fixation of 1000 ms during which the response was made. The duration of each block was 18-s. The total duration for each run was 250-s There was a 10-s resting period after the first run and before the second run begun.

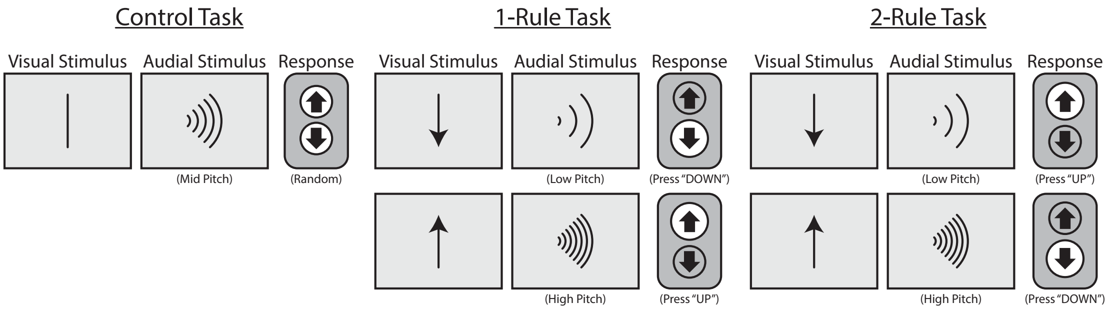

Figure 3-1 Visual and audial version of the Arrow Task

Reaction Time Measures

The mean reaction times for each of the six conditions were calculated. For the rest of the thesis, the reaction times for the control conditions will be termed "control RT", and the reaction times of the four stimulus-response mapping tasks will be termed "mapping RT". Trials with response time below 150ms were omitted from the calculation of mean RT and accuracy rate, and if omitted trials were more than 40%, the participants were omitted from the study. Participants with accuracy rate below 70% in any task condition were excluded from the analysis. The choice of 70% as cut-off was to ensure the correct responses would not have been due to random chance.

The mean reaction time for each task condition was entered in a 2 (group) × 2 (modalities) × 3 (task conditions) linear mixed model using the R package lme4, and subject was entered to the model as random effect. Significant main and interaction effects were followed with post-hoc analysis using the R package multcomp, with p-level corrected with Tukey's procedure.

MRI Scanning Parameters and Data Pre-processing

MRI images were acquired using GE Signa HDxt 3T scanner (General Electric, Milwaukee, WI, USA) with 8-channel phased-array head coil. High-resolution T1-weighted images were acquired using magnetization-prepared rapid gradient-echo (MP-RAGE) sequence (Axial acquisition, field-of-view 240 x 240 mm, slice thickness 1 mm without gap, 160 slices, acquisition matrix 256 x 256, TR 5556 ms, TE 1764 ms, inversion time 450 ms, flip angle 15 degree). During both auditory and visual task, 175 volumes of BOLD-fMRI images were acquired using T2*-weighted echo-planar imaging (EPI) sequence (Axial acquisition, field-of-view 240 x 240 mm, slice thickness 4mm without gap, 40 slices per volume, acquisition matrix 64 x 64, TR 2000 ms, TE 30 ms, 175 volumes, flip angle 90 degree).

Functional data were preprocessed with FMRIB Software Library (FSL version 5.0.9, (Jenkinson, Beckmann, Behrens, Woolrich, & Smith, 2012; S. M. Smith et al., 2004). In each run, first five volumes of the fMRI time series were removed to minimize magnetic field instability. The remaining 170 volumes were high-pass filtered with frequency 1/90 Hz to remove scanner drifting. The volumes were then rigidly aligned to the middle volume to correct for movement artifact. Gaussian spatial filter of 5mm full-width-half-maximum was applied. The images were then decomposed into independent components using FSL/MELODIC (Multivariate

Exploratory Linear Optimized Decomposition into Independent Components) with single-session Independent Component Analysis (ICA) option. Components were visually inspected using FSL/melview and classified as signal and different artifacts (R. E. Kelly et al., 2010). Denoised sessions were analyzed with general linear model, for which boxcar function for the three task conditions were convoluted with haemodynamic response functions. Temporal derivatives and motion parameters were entered to the model as additional regressors. Three task contrasts (Control, 1-Rule and 2-Rule) and two difference contrasts (1-Rule minus Control and 2-Rule minus Control) were obtained for subsequent group analyses.

Spatial coregistration from functional space to structural space, and normalization from structural space to MNI template space were performed using Advanced Normalization Tools (ANTs) version 2.2.0 (Avants et al., 2014). The mean functional image obtained from FSL preprocessing described above, and it was then corrected for intensity inhomogeneity introduced by bias field using N4BiasFieldCorrection. The rigid-body transformation matrix was calculated using the script antsIntermodalityIntrasubject.sh using default settings. Structural-to-template deformations were obtained using the script antsRegistrationSyN.sh using default parameters. SyN is a high dimension diffeomorphic registration algorithm (Avants, Epstein, Grossman, & Gee, 2008) which achieved highest rank among existing tools (Klein et al., 2009).

Identifying Common Neural Substrates: Conjunction analysis

To identify neural substrates which were engaged in all the four experimental conditions, conjunction analyses were conducted. The contrasts (COPE) and variance (VARCOPE) of the first level parameter estimates (1-Rule minus Control, 2-Rule minus Control, for both audial and visual modalities) were normalized to template space by merging functional-to-structural transformation and structural-to-template deformations in the previous step. They were then analyzed using FSL/FEAT using FLAME 1 higher level mixed-effect analysis in four separate models. To account for differences in group variance between younger and older group and imbalance number of participants, the two groups were modelled as different subject groups. Two explanatory variables were specified for each group to obtain the mean activation. Two contrasts were specified to capture the group mean for younger and older group separately. The activation maps for the 4 experimental conditions for both groups were entered into a conjunction analysis (Nichols, Brett, Andersson, Wager, & Poline, 2005). However, since the aim for this step was not to make statistical inference but to assist the selection of ROI, the conjunction map was only created by thresholding the voxel significance at $Z>2.3$, and no cluster-wise correction was performed. Since there would be differences in the activations in the younger and older group, the conjunction analysis was performed separately in each group. The maps from the younger and older group were then analyzed qualitatively, as the aim of this step was not to compare the differences in group activation, but only to serve the selection of ROI.

Cerebrum and Cerebellum Parcellation and ROI selection

To avoid bias towards a specific task and a specific group, I used the conjunction map to inform the selection of anatomically defined ROI. The structural images for each subject was parcellated using Human Connectome Project Multimodal Parcellation (Glasser et al., 2016), HCP-MMP version 1.0, downloaded from https://balsa.wustl.edu/WN56) and Cerebellum Lobule Segmentation Using

Graph Cuts (Yang et al., 2016), downloaded from http://www.iacl.ece.jhu.edu/index.php/Resources). The former parcellated the cerebral cortex into 180 regions by obtaining sharp boundaries using cortical structure, task fMRI, functional connectivity and myelination. Previous parcellation schemes used only structural landmarks to identify the boundaries for parcellation, without acknowledging the functional segregations. The latter parcellated the cerebellum into 22 regions by integrating multi-atlas labeling (15 hand-labelled T1 images), tissue classification and boundary classification using graph cut to achieve better segmentation accuracy. The T1 structural images were subjected to surface reconstruction using Freesurfer version 5.3.0 (Fischl & Dale, 2000). The HCP-MMP template was converted to Freesurfer fsaverage template, and then projected onto each individual subject. The cerebellum segmentation algorithm also required reconstructed surface from Freesurfer. The classifier was trained with the 15 hand-labelled images come with the software package. The same procedure was also performed on the MNI template for ROI selection. After the MNI template was parcellated, the parcellation map was overlaid on the binarized conjunction map for ROI selection. Selected ROIs were used to extract first level parameter estimates of task activation and extract timeseries for effective connectivity coefficient estimation as described below.

Activation Estimation

After the parcellations were selected as ROIs, the mean parameter estimates from the first level activation analysis task contrasts (1-rule and 2-rule versus implicit baseline) were extracted from each subject space. The parcellation masks were inversely transformed from structural space back to functional space using ANTs with the transformation matrix generated in previous step. The parameter estimates were extracted from the contrast images (COPE), and the mean values were calculated within each of the selected mask.

Effective Connectivity Estimation – Vector Auto-Regressive Modelling

The strength of effective connectivity was estimated with vector auto-regressive modelling (VAR) using 1dGC.R (G. Chen et al., 2011) from AFNI. VAR was a causality analysis method which could be regarded as a multivariate version of Granger Causality (Granger, 1969). The idea behind the causality inference was, between two timeseries A and B, A "Granger caused" B if A demonstrated a temporal correlation with a lagged (or delayed) version of B, and the correlation with the lagged B was higher than the correlation with non-lagged (the original timeseries) of B. VAR, instead of only bivariate relationship between two timeseries, it took multiple timeseries into account. Since the brain regions were interconnected, the fluctuation in region was influenced by the its own current state and the signal coming from multiple neural substrates. Hence, VAR could uncover causal influence masked by multiple sources, and at the same time reduce the effect of common cause.

Raw functional MRI data for each session was preprocessed with only motion correction and spatial smoothing with 5mm FWHM. As suggested by the author, the signal drifting was better removed with polynomial nuisance regressors, as bandpass filtering would introduce irregularities to the signal and possibly create spurious results. The path coefficients were first estimated from each of the four experimental condition. First, the mean signal within the ROI for each timepoint in the timeseries extracted from the mask generated from the previous step. Those timeseries were enter to the model as target variables. Haemodynamic response function was convoluted to the boxcar function to create regressors to remove the irrelevant timepoints. For example, to estimate the path coefficient of 1-Rule condition, the regressors for resting block, control block and 2-rule block, the movement regressors and the polynomial drifting regressors were entered to the model as nuisance variable. Conceptually, this was similar to psychophysiological interaction (PPI), but there was lagging in the timeseries. The stationery of timeseries were examined, and the degree of lagging was determined to be 1 TR with AIC criteria.

After the session-level analysis, the path coefficients and t-statistics estimated were subjected to a group level analysis, and paths with p-value less than 0.0001 were to be selected for subsequent analysis. There was two reason for choosing a stringent *p*-value. First, the significance values were not corrected for the VAR and the number of paths to be estimated was huge, as the number of paths would be the square of the number of ROI. For instance, if 15 ROIs were selected, there would be 225 pairwise connections. Therefore, a smaller number of more robust paths were selected for subsequent variable selection procedure.

Quantification of Speed – Time Indices

Three time indices (TIs) were derived from the response-mapping reaction times for the regression analyses: processing (PTI), sensorimotor (STI) and cognitive (CTI). The concept underling these times indices is to dissect the mapping RT into two compartments: time to complete decision processes and time to complete non-decision processes (Jensen & Reed, 1990). Non-decision time was defined as the time involved in carrying out the perceptual processes associated with the incoming stimuli and selecting and executing the motor response. Decision time was defined as the time involved in carrying out operations related to the 1- and 2-rule decisions. PTIs therefore were standard scores of mapping RTs; while STIs were standard scores on control RTs. CTIs were the standard score of residuals in terms of standard scores after the control RT were partialled out from the mapping RT using the following linear mixed model (Jensen, 2006):

$$Y_{ij} = x_{ij}^{t}\beta + u_{ij}^{t}\gamma_{i} + \epsilon_{ij}$$

where Y_{ij}=mean RT of the experimental task of j^{th} subject of task i, x=mean RT of the control task of j^{th} subject of task i, u=random effect factor for task condition (Modality x Task, factor with 4 levels), ϵ_{ij}=residual of j^{th} subject of task i. The residulization procedure ensured that STI and CTI were statistically orthogonal to each other, and therefore there were zero correlations between two indices. The time indices were normalized as a standard procedure for lasso regression (Tibshirani, 2011). Model fitting was done with R package lme4 to obtain the residuals.

Reaction time of the Arrow Task, equivalent to the PTI of the current study, has been used in various studies to examine the RT-activation correlates, such as go/no-go (Barber, Pekar, & Mostofsky, 2016), stimulus-response congruency (Barber & Carter, 2004), stimulus-stimulus congruency (K. Kim, Carp, Fitzgerald, Taylor, & Weissman, 2013), oddball (H. Kim, 2014), spatial-cueing (Domagalik, Beldzik, Oginska, Marek, & Fafrowicz, 2014), N-back (Takeuchi et al., 2012) and digit-symbol task (Rypma et al., 2006). In general, cognitive control regions demonstrated RT-related activations, suggesting that the activation of regions associated with supervisory processes. It is likely due to the activation of those regions sustained through the sensory input stage, processing stage, and motor output stage. The activation of stage-specific regions, however, could tend to engage in a fraction of the entire reaction time period, in other word, those regions demonstrated phasic engagement.

The CTI was designated to capture the processing time with sensorimotor time suppressed, and the statistical procedure "residualization" was applied. Previous studies adapted residualization to study brain correlates. For example, to study the structural correlates of cerebellum in motor and cognitive function, Kansal et al. administered 9 pairs of tasks to their subjects. To isolate a specific cognitive domain, the performance of a control task was regressed from the intended task. Take the trail making task for example, they administered TMT-A (connecting numbers in ascending sequence i.e. 1-2-3-…) and TMT-B (connecting alternate number and alphabet, i.e. 1-A-2-B…) to their subjects. The intended measure for TMT-A was visual search speed while TMT-B included an addition component of executive function. They regressed TMT-A scores from TMT-B scores to establish a cleaner measure of executive function domain. After establishing the adjusted scores for a particular domain, they did a sparse partial lease square on the cerebellar sub-region volumes to establish domain-specific correlates. Given that the stimulus-response mapping conditions of the Arrow task involved both sensorimotor and cognitive (stimulus-response rule mapping) components, and the control condition (simple reaction time) incorporated mainly sensorimotor components without processing of stimulus-response rule, should be a better measure of the cognitive processing speed than the measures used in previous studies, such as reaction time (Rypma et al., 2006), accuracy rate (Forn et al., 2009) and composite score calculated with reaction time and accuracy rate (Motes et al., 2013). The residualized score constitute the time to make the mapping decision, i.e. "cognitive time index (CTI)".

The STI, which was literally the reaction times of the control task (i.e. simple RT task), was also included in the analysis. The STI played a less important role in the current study. The main reason for including the index is for the completeness of the analysis. In Barber and colleague’s (2016) study, they also reported the RT-activation of a simple RT task, and the regions involved visual cortex and motor cortex, but not control- or attention-related regions. Hence, the simple RT task could have been relied solely on sensorimotor processes, and the response could be completed automatically, without heavy involvement of cognitive control and attention processes. In other words, the STI should have captured only automatic aspects of the sensorimotor components of the stimulus-to-response process.

Linear Mixed-effect Model and Variable Selection

Mixed-effects model was fitted for predictions of the three speed indices (PTI, STI and CTI) with brain activations and path coefficients as fixed effects, and experimental conditions (Audial 1-Rule, Visual 1-Rule, Audial 2-Rule and Visual 2-Rule) as random effects. A previous study also used multiple regression to predict response time from regional activations (Madden, Whiting, Provenzale, & Huettel, 2004). For all linear mixed-effects model regression analysis, we adopted the “least absolute shrinkage and selection operator” (lasso) in the variable selection instead of stepwise regression (Madden et al., 2004), which is meant to enhance prediction accuracy and interpretability (Groll & Tutz, 2014; Tibshirani, 1996). The main aim for using lasso was to identify the most informative predictors to describe the individual differences. Lasso was also found useful for controlling the possible overfitting problems arisen throughout the procedure and therefore it was preferred over stepwise regression (McNeish, 2015). Linear mixed model lasso regressions were performed using R package glmmlasso (Groll & Tutz, 2014). Since we are interested in the commonalities among all experimental conditions, the task condition was entered to the model as random effect. All predictors were normalized before model fitting. Optimal regularization parameter λ was determined iteratively from 100 to 1 with step size of 1, and the model with smallest AIC value was selected. Coefficients for all parameters were shrunk to 0 with λ equals 100 in the current study. To further improve potential instability of the variable selection, the variable inclusion probability procedure was applied (Bunea et al., 2011). The lasso regression was repeated with 5000 bootstrap sample, and the probability of selecting a particular variable were counted. Those predictors passed 50% probability were then regarded as selected predictors.

Predictors retained in the reduced models were random effects using restricted maximum likelihood with R package lme4, as coefficients estimated by lasso would bias towards zero (Hastie, Tibshirani, & Friedman, 2008). For each predictor, 95% confidence interval were calculated using parametric bootstrap with 1000 simulations, local effect sizes were calculated with Cohen's f^2 (Selya, Rose, Dierker, Hedeker, & Mermelstein, 2012). Marginal R^2 for all reduced models were obtained with R package MuMIn. Significance of overall models were estimated by comparing the reduced model with corresponding null models which contained only intercept and random effects.

Six models were constructed for each group of the subjects. For each of the time indices (Processing Time Index, Sensorimotor Time Index, Cognitive Time

Index), a set of activation predictors and a set of path predictors were subject to the variable selection procedure.

Chapter 4 Behavioral Results

The behavioral measures in terms of reaction times and accuracy rates are presented in Figure 4-1 and Table 4-1. The reaction times in here refer to raw behavioral data collected from the subjects when they performed the 6 task conditions inside the scanner. A linear mixed model was performed to investigate the effect of the Group, Modality, Task effects and their interactions with subject as random effect to correct for the repeated measures on the variables of interest. For reaction times, there was a significant main effect of Group (F(1,52)=20.59, *p*<0.0001) and Task (F(1,260)=275.8, p<0.0001), while the main effect of Modality (F(1,260)=0.05, *p*=0.81) was not statistically significant. The following interaction effects were significant: Group × Task (F(2,260)=8.05, *p*<0.001) and Modality × Task (F(2,260)=5.54, *p*=0.004). Others were not statistically significant Group × Modality (F(2,260)=2.07, *p*=0.15) and Group × Modality × Task (F(2,260)=2.31, *p*=0.10). Post-hoc test corrected with Tukey procedure on Group and Task showed that the older group had significantly slower reaction times than the younger group (β=41.03, *p*=0.03), the 1-Rule condition had reaction times significantly slower than the control condition (β=142.1, *p*<0.0001), and the 2-rule condition had significantly slower reaction times than the 1-Rule condition (β=32.9, *p*=0.0033). Further post-hoc tests were performed to compare the differences in the reaction times by each of the six conditions. The older participants were not significantly slower than younger group in the audial control (β=41.03, *p*=0.09) and visual control conditions (β=31.57, *p*=0.28). The older participants were significantly slower than their younger counterparts in the audial 1-Rule (β=62.71.03, *p*=0.002), audial 2-Rule (β=72.72, *p*<0.001), visual 1-Rule (β=63.36, *p*<0.002) and visual 2-Rule conditions (β=105.87, *p*<0.001).

Accuracy Rate

In the control task, since the participants were not required to make a judgement based on the task rules in the other experimental conditions, response rate was used to describe the reaction times yielded. For simplicity, response rate in the control task was referred as accuracy rate in the text below. For accuracy rate, there was a significant main effect of Task (F(2,260)=42.0, *p*<0.0001). Main effects of Group (F(1,52)=1.60, p=0.21) and Modality (F(1,260)=0.25, *p*=0.62) were not significant. The Group × Task (F(2,260)=6.06, *p*=0.002), Modality × Task (F(2,260)=3.37,*p*=0.035) and Group × Modality × Task (F(2,260)=3.317,*p*=0.038) were significant. The Group × Modality (F(2,260)=2.61, *p*=0.107) was not statistically significant. Post-hoc analysis on the task effect with Tukey procedure showed that the accuracy rates for the 1-rule and 2-rule conditions were significantly lower than the control condition (β=4.08, *p*<0.001, 2-rule: β=3.8, *p*=0.003). Another post-hoc analysis on Modality × Task effect on the older group showed that the accuracy rate of the visual 2-Rule condition was significantly lower than those of the other conditions for the older group (β=4.20-8.73, *p*<0.01).

Table 4-1 Behavioral measures of the Arrow Task performance. See also Figure 4-1 for visualization.

		Younger (N=34)				**Older (N=20)**			
		Auditory		**Visual**		**Auditory**		**Visual**	
	Task	**Mean**	**SD**	**Mean**	**SD**	**Mean**	**SD**	**Mean**	**SD**
Reaction Time (ms)	Control	310	77.8	308	51	351	71.5	339	73.6
	1-Rule	452	65.2	428	47.1	514	50	501	65.6
	2-Rule	485	67.1	485	54.2	548	60	591	72.8
Accuracy (%)	Control	100	0	100	0	100	0	100	0
	1-Rule	95.9	6.48	96.8	4.66	96.3	6.39	97.6	3.03
	2-Rule	96.2	3.73	96.8	2.82	95.5	6	91.3	8.88

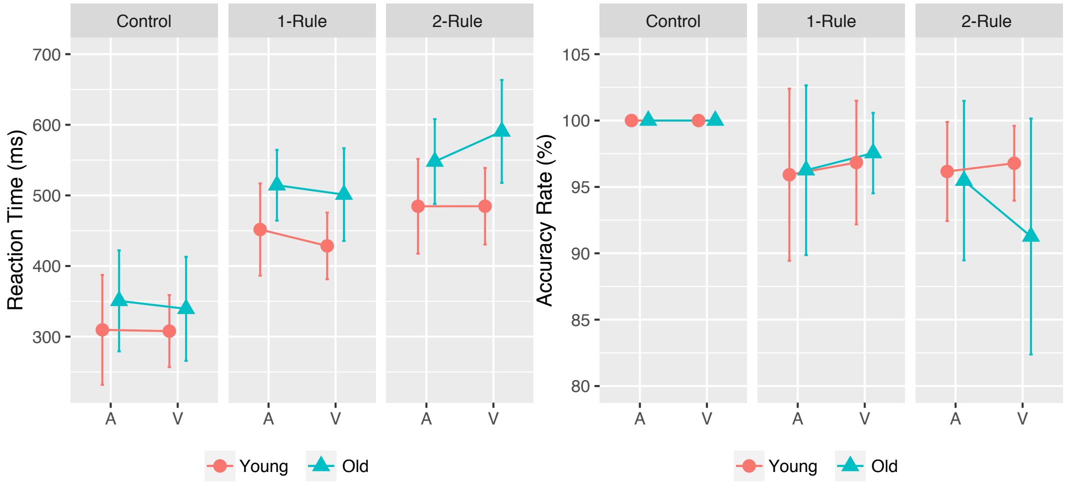

Figure 4-1 Behavioral performance of the Arrow task by younger and older group

Speed-Accuracy Tradeoff

Possible speed-accuracy tradeoff of the behavioral measures was examined using simple correlation test (Figure 4-2,Table 4-2). For the younger group, no significant reaction time-accuracy correlations were revealed (r<0.04 and *p*>0.05 for all conditions). For the older group, although the correlation coefficients for the 1-Rule conditions were moderate, they were not statistically significant (r=0.42, *p*=0.0655 for audial, r=0.44, *p*=0.0502 for visual).

Table 4-2 Correlation tests between reaction time and accuracy for each condition

		Younger		**Older**	
		r	p	r	p
Audial	Control	-	-	-	-
	1-Rule	0.00	0.997	0.42	0.0655
	2-Rule	0.01	0.939	0.21	0.3827
Visual	Control	-	-	-	-
	1-Rule	0.03	0.855	0.44	0.0502
	2-Rule	-0.02	0.905	0.17	0.4790

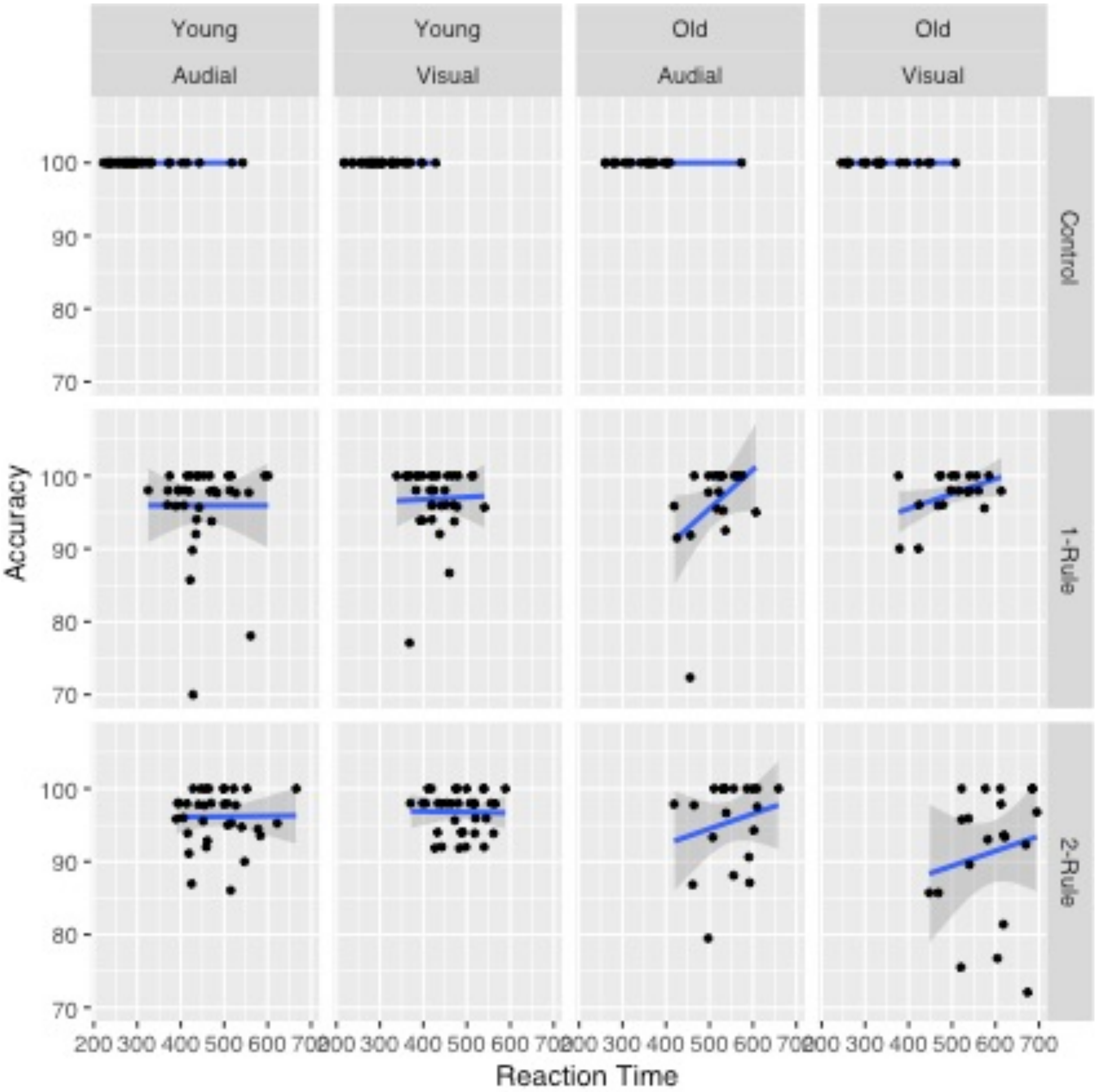

Figure 4-2 Scatter plot with regression lines for reaction time and accuracy

Discussion

Consistent with the results of Lee et al.'s (2006) study and of other studies that used stimulus-response compatibility tasks (Cieslik, Zilles, Kurth, & Eickhoff, 2010), the RT for the 2-rule condition (incompatible response) was significantly larger than that for the 1-rule condition (compatible response). This suggests that the 1-rule and 2-rule tasks recruited different cognitive processes, which supports our goal of identifying the neural substrates associated with processing speed. It is noteworthy that no significant differences were observed in the RTs (in either the younger or the older group) due to perceptions of the audial and visual modalities in the control condition. However, differences were observed between the two age groups in terms of performance in the 1-rule and 2-rule conditions. Verhaeghen (2013b) conducted a meta-analysis on the behavioral performance of the aging population and concluded that simple sensorimotor tasks that involve no decision component show little or even no age-related slowing. This result suggests that aging does not affect processing speed for basic sensory and simple motor tasks, such as the simple RT task in this study's control condition. This result further supports the validity of splitting the mapping RT into individual components and then conducting comparisons between younger and older groups. In the subsequent analyses, the control RT was used as a suppressor of the RT measures so as to partial out the time spent on the sensory and motor processes during the tasks. As there were no significant differences between the younger and older groups, the variation of the simple RT was likely due to individual differences among the participants in terms of psychophysical processing. Therefore, after subtracting the control RT from the mapping RT, the result could be an estimate of the cognitive processing time.

Chapter 5 Conjunction Analysis and Region of Interest Selection

Introduction

This chapter describes the procedures to identify the region of interest for subsequent best predictor selection. The task-independent activation map for both the younger and older groups were used to guide the selection of the anatomically defined regions. The results of the conjunction analyses and the selected ROIs are described.

Conjunction Analysis

Three conjunction analyses were performed to locate the modality- and task-independent activation regions in the younger and older group, and their overlapping regions. Four task contrasts (Audial 1-Rule minus Control, Visual 1-Rule minus Control, Audial 2-Rule minus Control and Visual 2-Rule minus Control) were entered into the conjunction analysis (Table 5-1and Figure 5-1). For the younger group, the bilateral superior frontal junction (or commonly referred to as frontal eye-field), bilateral superior medial cortex (including pre-supplementary motor area and anterior cingulate), anterior insula, intraparietal sulcus, cerebellar lobule 6/8 and cerebellar vermis were significantly activated in all the task conditions, except that the activations in the right intraparietal sulcus and bilateral anterior insula were not statistically significant after the cluster-wise FWE correction.

In the older group, the activation patterns observed were by and large similar to those of the younger group, except in the left anterior insula of which the activation was not statistically significant at the voxel z threshold of 2.3. In some regions, the older participants were observed to recruit similar neural substrates but to a wider spatial extent. Those regions included the bilateral superior frontal junction extending along the precentral sulcus to the inferior frontal junction, medial frontal cortex, and bilateral intraparietal sulcus. In other regions, the older participants recruited the similar cluster but to a lesser spatial extent than the younger participants. Those substrates included the right anterior insula and the bilateral cerebellum lobule 6, crus 1 and 8, and vermis.

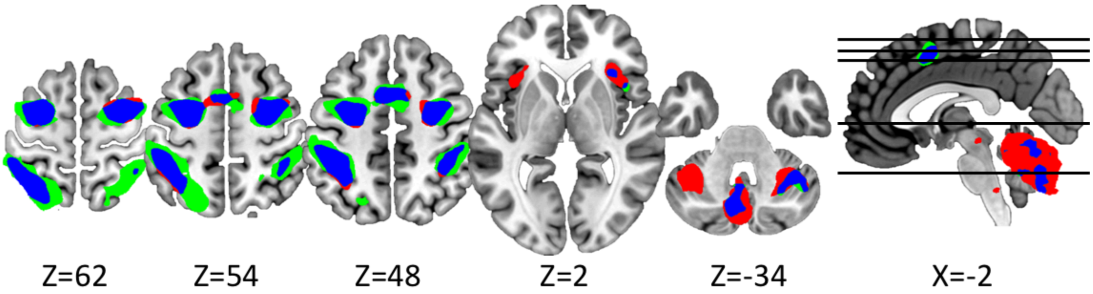

Figure 5-1 Conjunction Maps for Younger and Older group and Their Overlapping Area.

Red: conjunction map of 4 experimental contrasts (task-control) for the younger group, green: the same map for the older group, blue: overall conjunction map of all experimental contrasts for both groups

Table 5-1 Conjunction analysis for all task contrasts of younger and older group

Contrasts / Region	Lateral	Volume (Vox)	Cluster -log(p)	Peak Z	Peak MNI		
					X	Y	Z
Conjunction Map of Younger group							
Cerebellum Vermis, Left Lobule 6, 8, Right Lobule 8	B	4445	11.3	5.26	0	-66	-18
Left Intraparietal Sulcus	L	2200	6.38	5.08	-42	-42	50
Left Superior Frontal Junction, Bilateral Medial Frontal Cortex	L	1717	5.12	5.76	-28	-6	48
Right Superior Frontal Junction	R	1284	3.89	4.67	28	-2	58
Right Intraparietal Sulcus	R	491	n.s.	3.7	38	-44	48
Right Insula	R	156	n.s.	4.02	32	24	2
Left Insula	L	122	n.s.	3.73	-36	16	4
Conjunction Map of Older group							
Left Intraparietal Sulcus	L	3313	9.77	4.37	-26	-66	58
Left Superior Frontal Junction, Bilateral Medial Frontal Cortex	L	2462	7.67	5.02	-28	-2	48
Right Superior Frontal Junction	R	1523	5.03	3.86	28	-4	46
Right Intraparietal Sulcus	R	1323	4.41	4.04	40	-48	54
Cerebellum Vermis, Left Lobule Crus 1, 8	L	842	2.75	3.87	-8	-70	-34
Cerebellum Right Lobule 6, Crus 1	R	188	n.s.	3.48	42	-56	-32
Right Anterior Insula	R	92	n.s.	3.03	44	12	2
Cerebellum 8R	R	67	n.s.	2.92	18	-64	-58
Conjunction Map of both Younger and Older group							
Left Intra-parietal Sulcus	L	1924	5.95	3.94	-28	-62	60
Left Superior Frontal Junction	L	1132	3.59	4.86	-28	-2	50
Right Superior Frontal Junction	R	1054	3.34	3.86	28	-4	46
Cerebellum Vermis, Left Lobule 6, Crus 1, 8	L	601	1.7	3.87	-8	-70	-34
Right Intra-parietal Sulcus	R	405	n.s.	3.69	40	-42	48
Bilateral Medial Frontal Cortex	L	255	n.s.	3.64	-4	8	48
Cerebellum Right Lobule 6, Crus 1	R	145	n.s.	3.4	36	-48	-34
Cerebellum Left Lobule 6, Crus 1	L	126	n.s.	2.91	-36	-56	-30
Cerebellum Right Lobule 8	R	51	n.s.	2.77	16	-66	-56
Cerebellum Left Lobule 8	L	46	n.s.	2.74	-22	-60	-52
Right Insula	R	41	n.s.	2.99	32	24	2

Note: although the decision for region-of-interest selection did not reference to the cluster-wise significance test, a family-wise (FWE) correction was performed at voxel Z>2.3 and cluster p<0.05 for reference. n.s: not significant.

Cortical and Cerebellum Parcellations

The cortical parcellation generated from the Human Connectome Project was successfully projected on the Freesurfer fsaverage surface template (Figure 5-2). The parcellation was further projected on each particpant based on the surface-based registration. Surface reconstructions and projections were visually verified for quality.

The cortical labels were projected on the structural images. Figure 5-3 shows the result of one of the young participant . Parcellation of the cerebellum using multi-atlas labelling and graph cuts were also performed and visually checked, see also Figure 5-3 for an exemplar of the result. The same procedure was applied on the MNI template to guide the selection of ROIs.

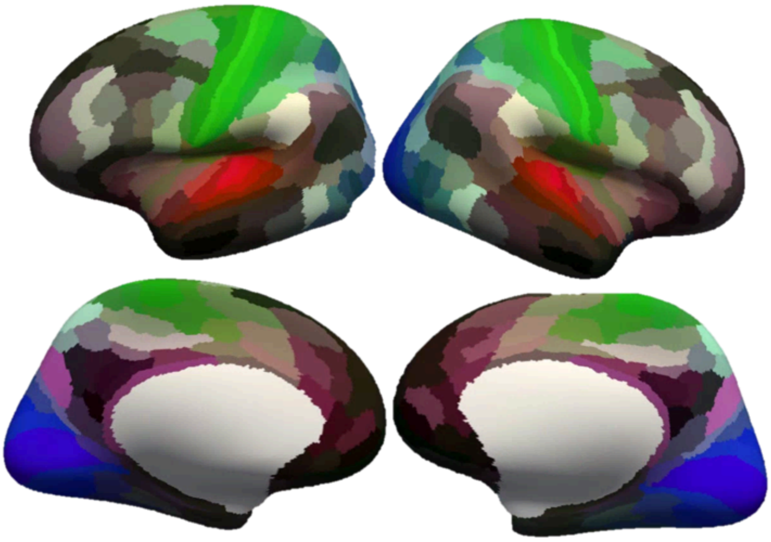

Figure 5-2 Projection of Human Connectome Project parcellations on Freesurfer template

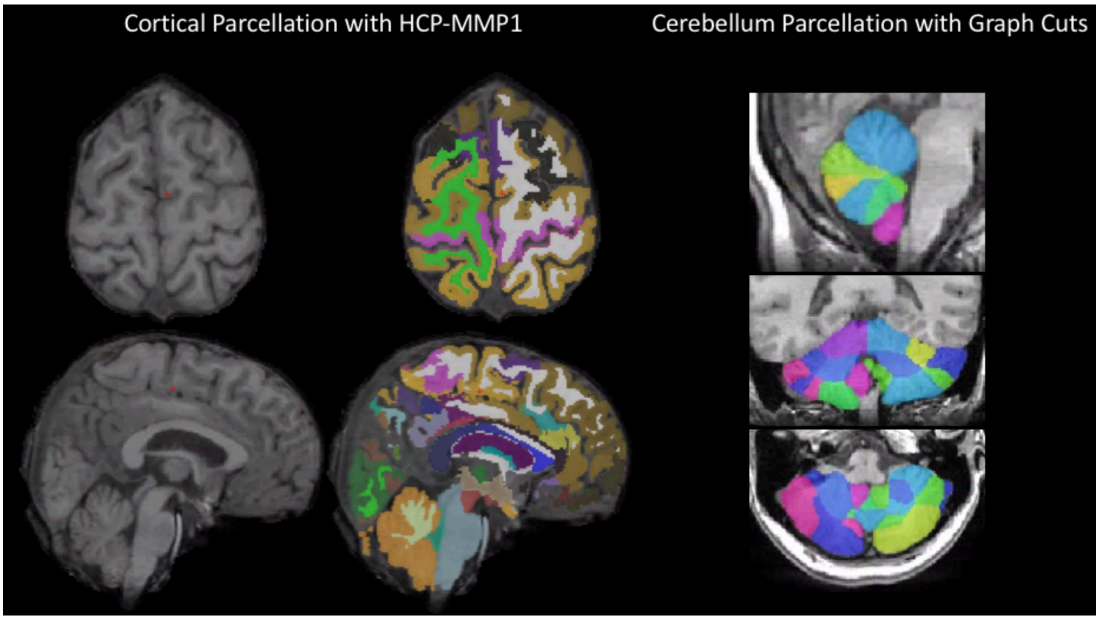

Figure 5-3 Final cortical and cerebellum parcellations on one subject.

Left: cortical parcellation with HCP-MM1 template. Right: Multi-atlas-based cerebellum parcellation with Graph Cuts.

ROI selection

Region-of-interests were selected based on visual inspection of the conjunction maps and the parcellations generated from the previous analytical procedures. Selected cortical parcellations for the medial frontal cortex were the LSCEF (left) and RSCEF (right), which appeared to cover the pre-supplementary motor area and anterior cingulate. For the superior frontal junction, L6a (left) and R6a (right) were selected, which was also referred to as frontal eye-field in the literature. For anterior insula, the LAVI (left) and RAVI (right) were selected. Although the older group did not show significant activation in the left anterior insula, it was still considered to be an important ROI as it was associated with the stable task-set maintenance network which involved medial prefrontal cortex which facilitated top-down control (Dosenbach, Fair, Cohen, Schlaggar, & Petersen, 2008). For intraparietal sulcus, two pairs of ROIs were selected due to the massive volume and functional segregation. Specifically, using a similar response-compatibility task, Cieslik and colleagues' study (2010) suggested that the anterior IPS facilitated top-down reorienting attention while more posterior part demonstrated bottom-up properties. For anterior IPS, LAIP (left) and RAIP (right) were selected, while LLIPv (left) and RLIPv (right) were selected for posterior IPS. Although left posterior IPS was not significantly activated in the younger group, the ROI was also entered in the subsequent analysis to facilitate comparison for younger and older group. For cerebellum, vermis VI/VII/VIII were selected. It was selected as the activation in the vermis was the highest in the cerebellum in both groups. Also, vermis size was consistently related to cognitive decline in aging populations (Bernard, Leopold, Calhoun, & Mittal, 2015; Miller et al., 2013; Paul et al., 2009). Selected ROIs were overlaid on MNI template for visualization (Figure 5-4). The extraction of timeseries and parameter estimates were performed on individual subjects' parcellation maps.

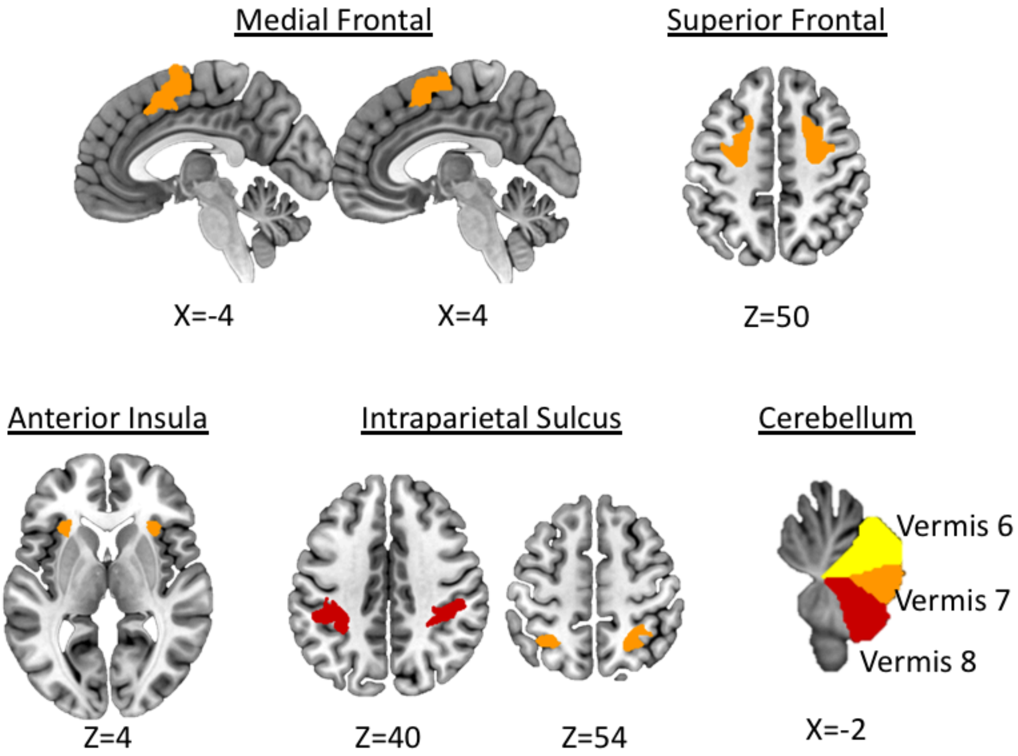

Figure 5-4 Region of Interests Selected from Anatomically Defined Regions.

LSCEF: left medial frontal, L6a: left superior frontal junction, LAVI: left insula, LAIP: left anterior intraparietal, LLIPv: left posterior intraparietal, RSCEF: Right medial frontal, R6a: right superior frontal junction, RAVI: right insula, RAIP: right anterior intraparietal, RLIPv: right posterior intraparietal, CV6/7/8: Cerebellum Vermis VI/VII/VIII. Labels for cortical ROIs were adapted from HCP-mmp1 atlas.

Discussion

The conjunction analyses revealed the neural substrates that were grouped under a common network for all the task conditions: the bilateral SFJ, MFC, anterior insula, intraparietal sulcus, and cerebellum. The MFC and bilateral insula have been associated with stable cognitive control, which mediates task-set maintenance to facilitate goal-related behavior (Dosenbach et al., 2008; Petersen & Posner, 2012).

The bilateral SFJ and intraparietal sulcus have been known to serve top-down attention functions (Corbetta & Shulman, 2002; Corbetta, Patel, & Shulman, 2008), and together, they are known as the dorsal attention network. The activations of the cerebellar vermis in this study are consistent with those in other studies involving sustained attention during simple cognitive tasks (see Langner & Eickhoff, 2013 for review and meta-analysis). In particular, Langner et al. (2013) suggested that the vermis supported the preparatory and anticipation processes during the occurrence of an event. Regions related to adaptive cognitive control, including the DLPFC and lateral parietal lobule (Vincent, Kahn, Snyder, Raichle, & Buckner, 2008), were not found to be statistically significant in this conjunction analysis, which suggests that the experimental tasks used in the study involved minimal adaptive cognitive control. The ROIs selected for this study, based on the stipulated analyses, provide useful information on the processing speed.

In a similar study of a spatial stimulus-response compatibility task (Cieslik et al., 2010), there were activations in the right temporoparietal junction—a part of the ventral attention network, which is responsible for bottom-up attention (Corbetta et al., 2008; Corbetta & Shulman, 2002). The postulate in this study is that the absence of temporoparietal junction activation in this task was grounded in a lack of overt spatial orientation. In their (Cieslik et al., 2010) experimental paradigm, the semantic representation was delivered in the visuospatial domain, with a red dot on either the left or right side of the screen; the subjects had to orient their attention to a spatial location and construct a modal-free representation from the spatial information. In this study, detecting and encoding the stimuli in both modality conditions should not have involved significant audio- or visuospatial orientation. For the visual stimuli, the arrow sign was always presented in the same location. For the audial stimuli, the sound was delivered to both ears simultaneously. Therefore, the current paradigm should have involved minimal spatial orientation, and the processing time related to the bottom-up orientation should have been minimized.

In summary, 13 ROIs were selected: the left and right regions of the MFC, SFJ, anterior insula, anterior intraparietal sulcus, and posterior intraparietal sulcus; as well as the cerebellum vermis VI, VII, and VIII.

Chapter 6 Neurophysiological Correlates of Processing Speed in the Younger Adult

Effective Connectivity Path Estimation

The timeseries of the 13 selected ROIs were extracted from the anatomically defined ROI in each younger participant's native space. They were analyzed with multivariate vector autoregression implemented in the 1dGC.R script from AFNI to estimate the path coefficients for the four experimental conditions (Audial/Visual 1-Rule/2-Rule) for each participant. The time series extracted from the ROIs passed both KPSS and ADF tests for their stationarity and met the AIC 1-TR (2s) degree of lagging criteria. Group analysis was then performed by entering path coefficients and p-values of all the four experimental conditions into 1dGC.R in group analysis mode. Among the 169 pairwise pathways, 13 self-loops were excluded from further analysis. Seventy-two out of the 157 effective connectivity paths passed the $p<0.00001$ threshold and selected for further analyses.

Nine ROIs showed significant causal influences on other brain regions in the younger group. Bilateral medial frontal ROIs (LSCEF, RSCEF), right anterior insula (RAVI), right anterior intraparietal sulcus (RAIP) and vermis VIII (CV8) showed positive causal influence to multiple brain regions, implying that the increased (or decreased) activations in the source regions caused an increase (or decrease) in the activations of the neural substrates in the destination regions among the younger participants. Right posterior intraparietal sulcus (RLIPv) and vermis VI (CV6) demonstrated negative influences on other regions. Left posterior intraparietal sulcus (LLIPv) and right superior frontal junction (R6a) showed mixed result, but both of them showed negative causal influence to their contralateral counterparts.

Table 6-1 Path coefficients of effective connectivity in the younger group

	CV6	**CV7**	**CV8**	**LSCEF**	**L6a**	**LAVI**	**LAIP**	**LLIPv**	**RSCEF**	**R6a**	**RAVI**	**RAIP**	**RLIPv**
CV6		0.044	0.057	**-0.114**	-0.082	**-0.080**	**-0.068**	**-0.145**	**-0.094**	**-0.104**	**-0.128**	**-0.129**	**-0.145**
CV7	0.005		-0.047	-0.044	-0.049	-0.028	-0.046	-0.014	-0.026	-0.042	-0.033	-0.047	-0.064
CV8	**0.136**	**0.080**		**0.058**	0.062	**0.044**	**0.044**	**0.057**	**0.044**	0.060	0.036	**0.049**	**0.070**
LSCEF	**0.209**	**0.162**	**0.186**		**0.274**	**0.164**	**0.168**	**0.174**	**0.093**	**0.316**	**0.215**	**0.143**	**0.148**
L6a	0.021	0.005	0.008	-0.027		-0.004	0.018	-0.006	-0.016	-0.046	-0.035	-0.031	-0.021
LAVI	-0.029	0.015	0.012	0.004	0.006		-0.056	-0.035	0.046	0.007	-0.069	-0.017	0.006
LAIP	0.033	-0.002	0.020	0.042	0.017	0.022		0.012	-0.053	-0.006	0.040	0.004	-0.012
LLIPv	**0.070**	0.030	0.026	-0.036	0.039	-0.006	0.000		-0.010	0.015	-0.035	**-0.077**	**-0.113**
RSCEF	**0.188**	**0.129**	**0.110**	**0.116**	**0.352**	0.070	0.052	0.090		**0.297**	**0.111**	**0.103**	**0.167**
R6a	-0.010	-0.025	-0.040	-0.009	**-0.079**	0.021	**0.033**	0.004	-0.013		0.029	0.026	0.017
RAVI	0.027	**0.053**	0.038	0.028	0.018	0.028	-0.005	0.023	0.034	**0.079**		**0.047**	**0.072**
RAIP	**0.138**	**0.135**	**0.118**	**0.177**	**0.213**	**0.124**	**0.108**	**0.138**	**0.103**	**0.288**	**0.184**		**0.642**
RLIPv	**-0.114**	**-0.105**	**-0.077**	**-0.150**	**-0.218**	**-0.094**	**-0.086**	**-0.098**	**-0.104**	**-0.219**	**-0.132**	**-0.170**	

Note: the table read from column to row. For example, index of the path from L6a to CV6 is the fifth row of the first column. Boldfaced path coefficients denoted $p<0.00001$. CV6/7/8: Cerebellum Vermis VI/VII/VIII, LSCEF: left medial frontal, L6a: left superior frontal junction, LAVI: left insula, LAIP: left anterior intraparietal, LLIPv: left posterior intraparietal, RSCEF: Right medial frontal, R6a: right superior frontal junction, RAVI: right insula, RAIP: right anterior intraparietal, RLIPv: right posterior intraparietal.

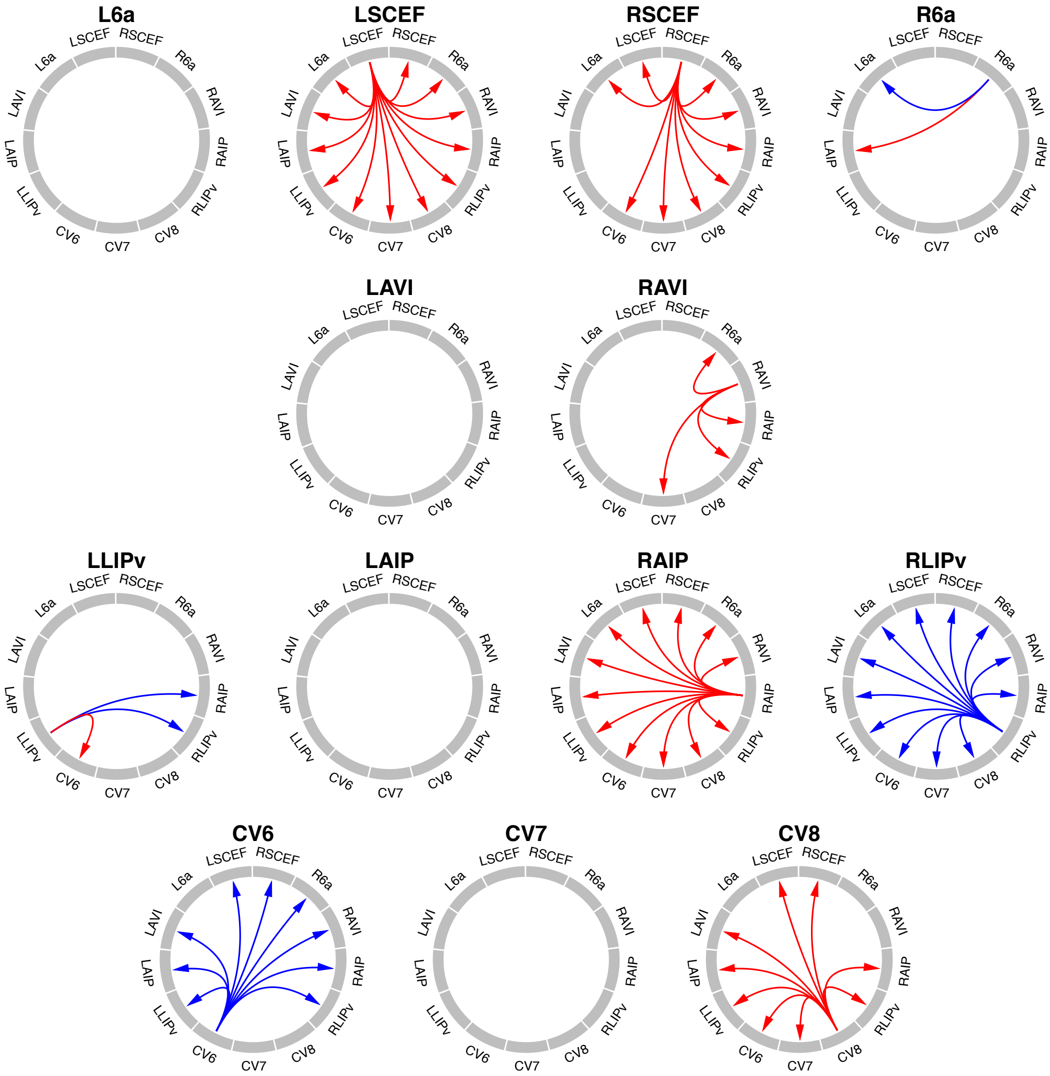

L6a LSCEF RSCEF R6a LAVI RAVI LLIPv LAIP RAIP RLIPv CV6 CV7 CV8

Figure 6-1 Diagram for the effective connectivity.

Each diagram was labelled with the source of the causal influence. Blue arrow: negative influence, higher (or lower) activation in the source region Granger caused a lower (or higher) activation in the destination region. Red arrow: positive causal influence, higher (or lower) activation in the source region Granger caused a higher (or lower) activations in the destination region.

Parameter estimates of the task activation contrast with implicit baseline for the four experimental conditions of 13 ROIs were subjected to three separate linear-mixed lasso regression model models. The results yielded were to predict the three time-indices in processing speed among the younger participants: PTI (processing), STI (sensorimotor) and CTI (cognitive). The final model which predicted the PTI was significant ($\chi^2(3)=17.208$, p=0.0006, $R^2=0.0998$), and it contained the cerebellar vermis VI ($f^2=0.248$, β=0.390, p=0.001), right medial frontal cortex ($f^2=0.204$, β=-0.249, $p=0.009$), and vermis VII ($f^2=0.197$, β=0.316, $p=0.011$). The final model predicted STI was significant ($\chi^2(3)=21.416$, p<0.0001, $R^2=0.1429$), and it involved left superior frontal junction (L6a)($f^2=0.16219$, β=-0.26719, $p=0.058$), right medial frontal cortex (RSCEF, $f^2=0.14098$, β=-0.20549, $p=0.096$), and left Intraparietal, Anterior (LAIP, $f^2=0.13438$, β=0.15998, $p=0.11$). However, the variables were not significant. The final model predicted CTI was significant ($\chi^2(4)=20.491$, $p=0.0004$, $R^2=0.1363$). It involved vermis VII ($f^2=0.377$, β=-0.56274, $p<0.001$), vermis VI ($f^2=0.29526$, β=0.43941, $p<0.001$) which were significant, and left superior frontal junction (L6a, $f^2=0.14424$, β=0.19981, $p=0.09$) and right superior frontal junction (R6a, $f^2=0$, β=-0.03976, $p=0.71$) which were not significant.

Speed-related connectivity analysis

Estimated 72 path coefficients were subjected to three separate models as explanatory variables to predict the three time-indices for the younger group as above. The final model which predicted PTI was significant ($\chi^2(2)=15.902$, p=0.0004, $R^2=0.0921$). Both selected paths right anterior intraparietal to vermis VII (RAIP to CV7, $f^2=0.25812$, β=-0.25583, $p=0.001$), and vermis VI to right superior frontal (CV6 to R6a, $f^2=0.21452$, β=-0.21217, $p=0.007$) were significant. The final model which predicted STI was significant ($\chi^2(3)=37.575$, $p<0.0001$, $R^2=0.2373$). The paths right anterior intraparietal sulcus to vermis VII (RAIP to CV7, $f^2=0.3042$, β=-0.27358, $p<0.001$), right medial frontal to right posterior intraparietal sulcus (RSCEF to RLIPv, $f^2=0.18972$, β=0.22844, $p=0.026$), and right medial frontal to Vermis VII (RSCEF to

CV7, $f^2=0.16899$, $\beta=0.20602$, $p=0.046$) were significant. The final model which predicted CTI was also significant ($\chi^2(2)=12.690$, $p=0.0017$, $R^2=0.0879$). The selected paths right superior frontal to left anterior intraparietal (R6a to LAIP, $f^2=0.20139$, $\beta=0.20009$, $p=0.02$), and right medial frontal to vermis VI (RSCEF to CV6, $f^2=0.18028$, $\beta=-0.17947$, $p=0.037$) were significant.

Table 6-2 Best predictors selected by lasso regression on three time-indices in the younger group

				95% CI		
Model / Selected Variable	f^2	**β**	**se**	**lwr**	**upr**	**P**
Younger group: Predict Processing Time Index (PTI) with Activations						
Cerebellar Vermis VI	0.248	0.390	0.120	0.166	0.639	0.001**
Right Medial Frontal Cortex (RSCEF)	0.204	-0.249	0.094	-0.439	-0.050	0.009**
Cerebellar Vermis VII	0.197	-0.316	0.123	-0.536	-0.071	0.011*
Model summary: $\chi^2(3)=17.208$, p=0.0006, $R^2=0.0998$						
Younger group: Predict Sensorimotor Time Index (STI) with Activations						
Left Superior Frontal Junction (L6a)	0.162	-0.267	0.140	-0.546	0.026	0.058.
Right Medial Frontal Cortex (RSCEF)	0.141	-0.205	0.123	-0.429	0.036	0.096.
Left Intraparietal, Anterior (LAIP)	0.134	0.160	0.100	-0.068	0.345	0.11
Model summary: $\chi^2(3)=21.416$, p<0.0001, $R^2=0.1429$						
Younger group: Predict Cognitive Time Index (CTI) with Activations						
Cerebellar Vermis VII	0.377	-0.563	0.128	-0.826	-0.284	<0.001***
Cerebellar Vermis VI	0.295	0.439	0.128	0.165	0.668	<0.001***
Left Superior Frontal Junction (L6a)	0.144	0.200	0.117	-0.010	0.443	0.09.
Right Superior Frontal Junction (R6a)	0.000	-0.040	0.108	-0.277	0.167	0.71
Model summary: $\chi^2(4)=20.491$, p=0.0004, $R^2=0.1363$						
Younger group: Predict Processing Time Index (PTI) with Connectivity						
Right Anterior Intraparietal (RAIP) to Vermis VII (CV7)	0.258	-0.256	0.077	-0.413	-0.118	0.001**
Vermis VI (CV6) to Right Superior Frontal (R6a)	0.215	-0.212	0.077	-0.369	-0.064	0.007**
Model summary: $\chi^2(2)=15.902$, p=0.0004, $R^2=0.0921$						
Younger group: Predict Sensorimotor Time Index (STI) with Connectivity						
Right Anterior Intraparietal (RAIP) to Vermis VII	0.304	-0.274	0.077	-0.425	-0.114	<0.001***
Right Medial Frontal (RSCEF) to Right Posterior Intraparietal (RLIPv)	0.190	0.228	0.102	0.021	0.406	0.026*
Right Medial Frontal (RSCEF) to Vermis VII (CV7)	0.169	0.206	0.102	0.018	0.401	0.046*
Model summary: $\chi^2(3)=37.575$, p<0.0001, $R^2=0.2373$						
Younger group: Predict Cognitive Time Index (CTI) with Connectivity						
Right Superior Frontal Junction (R6a) to Left Anterior Intraparietal (LAIP)	0.201	0.200	0.085	0.031	0.362	0.02*
Right Medial Frontal (RSCEF) to Vermis VI (CV6)	0.180	-0.179	0.085	-0.356	0.002	0.037*
Model summary: $\chi^2(2)=12.690$, p=0.0017, $R^2=0.0879$						

Note: f^2: effect size, se: standard error, lwr/upr: lower/upper bound at 95% confidence interval, *<0.05, **<0.01, ***<0.01

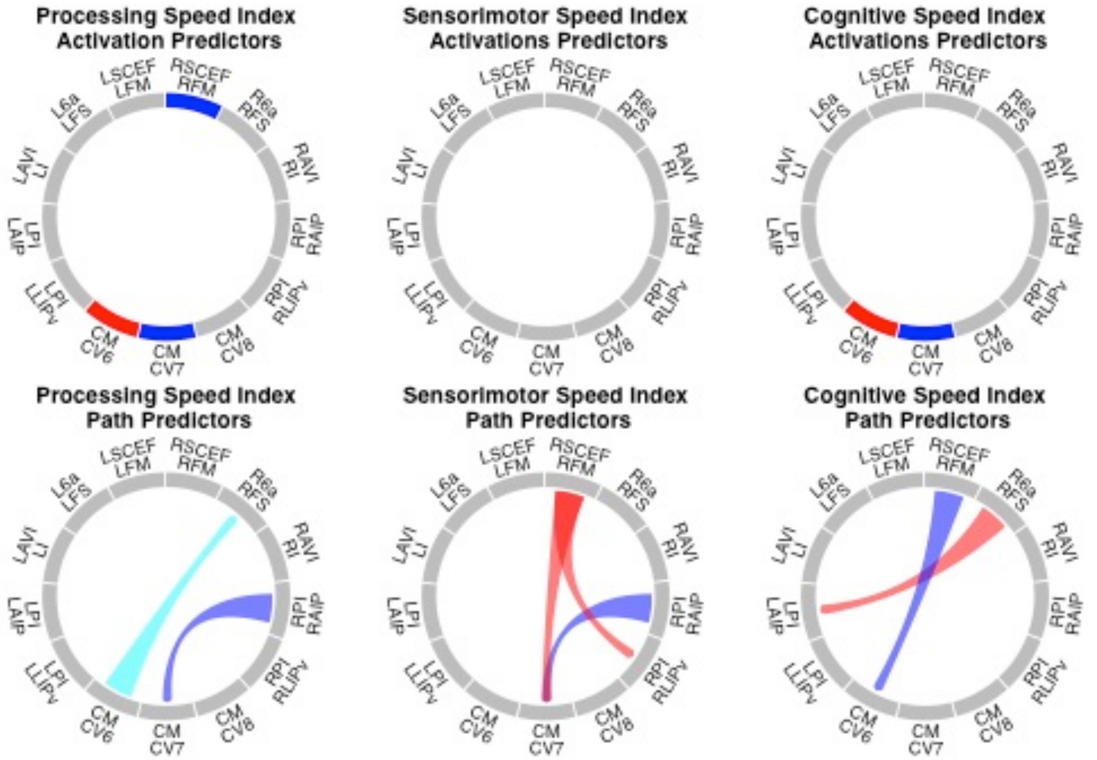

Figure 6-2 Significant activation and connectivity predictors selected by lasso regression in the younger group.

Note: Sections on the track represented the activation of the ROI. Blue: higher activation predicted shorter time. Red: higher activation predicted longer time. Arrows connecting different ROIs were the significant paths. Blue arrow: Decreased positive influence predicted longer time. Cyan arrow: Decreased negative influence predicted longer time. Red arrow: Increased positive influence predicted longer time.

Discussion

This study explored the mechanisms underlying processing speed by employing visual and audial stimuli in a simple response-selection paradigm. The results suggested the use of a common task-positive neural network composed of the bilateral MFC, bilateral anterior insula, bilateral SFJ, left intraparietal sulcus, and cerebellum. Effective connectivity analysis revealed that the bilateral MFC, right anterior insula, right anterior intraparietal sulcus, and cerebellum vermis VIII exerted positive causal influences on other substrates, suggesting that higher activations in one substrate caused higher activations in other substrates within the network (Figure 6-1,

Table 6-1). By contrast, the right posterior intraparietal sulcus and vermis VI exerted negative influences on the system. Additional analyses newly revealed the cerebellum's roles in influencing speed. Before the non-decision processes were partialled out, processing speed was associated with activations in the right medial PFC, vermis VI, and vermis VII, but only the latter two were retained in CTI. Of these activations, increases in the right MFC and vermis VII, as well as decreases in the vermis VI, were each independently associated with faster (smaller) CTI. These results suggest that vermis VII plays a facilitating role and that its activations are associated with faster (smaller) PTI and CTI. Second, the identified reciprocal fronto-parietal-cerebellar pathways were associated with decision speed. In particular, increased negative influence of the vermis VI on the right SFJ and decreased influence of the right anterior intraparietal sulcus on vermis VII were the best predictors of accelerated PTI. Faster CTI, on the other hand, was associated with increased positive influence of the right MFC on the left anterior intraparietal sulcus and by reduced positive influence of the right SFJ on the same region. Our findings suggest that interactions between the cognitive-control processes (mediated by the frontal neural substrates) and the control-to-automatic perceptual decision processes (mediated by the cerebellar neural substrates) play important roles in facilitating processing speed.

Justification for Variable Selection with the Three Time Indices

The CTI was derived by parceling out the control RT from the mapping RT so as to capture the time spent on the endogenous processes that are associated with mapping the stimulus-to-response rules. The validity of this method was substantiated via the clustering of the neural substrates associated with STI and CTI. The results of the regression analysis indicated that CTI was more strongly associated with activations of the focal neural substrates in the cerebellar vermis, whereas the MFC was not associated with decision speed once the non-decision component was removed. MFC activations have been shown to be best explained by the time-on-task effect, which describes the associations between response time and the intra-subject variability of brain activations (Carp, Fitzgerald, Taylor, & Weissman, 2012; Weissman & Carp, 2013). In particular, in those studies, congruency, stimulus–stimulus conflict, response conflict, and error effect were eliminated after controlling for response time. This suggests that the MFC plays a more general supervisory role in the entire task, which governed the sensory input stage, rule-based decision stage and motor stage. In other words, the activation of MFC begins at the onset of stimulus and sustains until completion of motor response and evaluation of the performance. Therefore, after removing the non-decision components, that is processing time spent on sensory and motor stages, the time spent on decision processing (estimated with CTI) was not significantly correlated with the activation of the MFC. In contrast, the vermis activations were not only remained associated to decision speed (CTI), but the beta estimates and effect sizes were also greater than that of the PTI. Therefore, it is asserted that CTI had captured the decision processes. For instance, the vermis VI/VII was considered to substantiate specific task processes such as oculomotor (Kleine, Guan, & Buttner, 2003), rule-based visuomotor decision making (Deverett, Koay, Oostland, & Wang, 2018; Owens et al., 2018), adaptive control (Herzfeld, Kojima, Soetedjo, & Shadmehr, 2018), and performance monitoring (Peterburs & Desmond, 2016). Consequentially, the speed-related activation results supported the partitioning of decision speed.

In addition, dividing RT into two orthogonal compartments (decision or non-decision) unmasked the brain-behavior relationships. In fact, the time spent on rule-based decision occupied around one-third of the entire processing time (under the assumption that the decision time = (Mapping RT - control RT)/Mapping RT). The covariance associated with the decision processing and activations could have been masked by the noise introduced by the variance of sensorimotor processing time. Right MFC connectivities were not sufficient predictors of PTI, but they did differentially contribute to non-decision speed (STI) and decision speed (CTI) after bootstrap resampling. Therefore, the method used in this study could be used to extract the decision component of processing speed or to unmask brain correlates by suppressing the non-decision components of speed.

Processing Speed of Stimulus-Response Rule Mapping

In this study, increased right MFC activation predicted accelerated processing speed (PTI). The MFC findings are consistent with those of previous studies, which further supports the positive speed-activation association across a variety of cognitive tasks: digit-symbol tasks (Forn, Ripollés, et al., 2013a), stop-signal tasks (C. S. R. Li, 2006), response-inhibition tasks (Wager et al., 2005), and simple sustained-attention tasks (Hilti et al., 2013). By comparing the brain activations of fast and slow performers using a simple sustained-attention task, Hilti and colleagues (2013) found that fast performers maintained higher MFC activations than slow performers. The function of the MFC in cognitive control has also been related to vigilance and alertness (Mottaghy et al., 2006), which was facilitated by task-set maintenance (Dosenbach et al., 2006). That conjecture matches with one of this study's hypotheses. Langner and colleagues (2011) also presented a vigilant (simple RT) task with three perceptual modalities (audial, visual, and vibrotactile), and they reported that the resulting network contained the MFC and vermis. That network was also reported in another meta-analysis that encompassed simple paradigms such as zero-back, go/no-go, and response-mapping tasks (Langner & Eickhoff, 2013). In addition, causal influence of the right MFC on vermis VI, vermis VII, and the right posterior intraparietal sulcus were associated with non-decision (STI) and decision (CTI) speed (Langner & Eickhoff, 2013). These findings further support the claim that the MFC plays a role in cognitive control.

In this study, activations in vermis VI and vermis VII were differentially associated with processing speed (PTI) and decision speed (CTI); these activations were the only activation predictor of decision speed. These results signify the importance of the cerebellar vermis in mediating the processes that are involved in a simple stimulus-response mapping task. Common attributions of the cerebellum's roles include an influence on general cognition (Koziol et al., 2014) and on the processing of auditory and visual information (Kansaku, Hanakawa, Wu, & Hallett, 2004; Langner et al., 2011). Specific to this study, a higher volume of vermis was correlated with faster RTs (Bernard & Seidler, 2013) and higher digit-symbol coding scores (Nadkarni et al., 2014); in addition, higher BOLD responses for the vermis (Rao, Motes, & Rypma, 2014) correlated with longer RTs on the digit-symbol task among younger adults. According to other researchers, the vermis also may play a role in the automaticity of a new action. For example, lesions in the vermis have been found to impair the habituation of new behaviors in mice (Callu, Puget, Faure, Guegan, & Massioui, 2007), and suppressive stimulation of the vermis has been shown to reverse the practice effect for a lexical-decision task in humans (Argyropoulos, Kimiskidis, & Papagiannopoulos, 2011). These results show that stronger activation of vermis VII predicts faster decision speed (smaller CTI) and processing speed (smaller PTI). Functionally, vermis VII has also been associated with adaptive cognitive control (Fan, McCandliss, Fossella, Flombaum, & Posner, 2005; Q. Li et al., 2015b; Weissman, Woldorff, Hazlett, & Mangun, 2002) and executive function (E, Chen, Ho, & Desmond, 2014). In particular, the vermis VII encodes a representation of mapping rules (Balsters et al., 2012). Structurally, in a viral tracing study in monkeys, a direct connection has been found between vermis VII and area 46 (R. M. Kelly & Strick, 2003), which is the equivalent of the DLPFC in humans. In a measure of resting-state functional connectivity in humans, vermis VII has been found to connect to the frontoparietal control network (Buckner, Krienen, Castellanos, Diaz, & Yeo, 2011; Habas et al., 2009). Thus, vermis VII was predicted to function as a counterpart of the frontoparietal control network.

These results suggest that lower activations in the vermis VI are associated with faster processing speed (smaller PTI) and decision speed (smaller CTI). In fact, vermis VI has been associated with response readiness (Langner et al., 2011), vigilant attention (Langner & Eickhoff, 2013), and the automatization of cognitive processes (Balsters et al., 2012; Callu, Lopez, & Massioui, 2013; Lang & Bastian, 2002). In resting-state functional connectivity studies, researchers (Buckner et al., 2011; Habas et al., 2009) have reported that vermis VI is functionally connected to the frontoinsular network, which has been associated with stable task-set maintenance (Dosenbach et al., 2007). For instance, to perform a task successfully, according to Dosenbach et al. (2006), the task-set maintenance system sends a top-down bias signal to engage the relevant input, processing, and output subsystems, and it then receives bottom-up feedback. In the mapping task in this study, the cognitive processes involved loading and maintaining appropriate mapping rules, attending to mental representations in the sensory cortex, binding the stimulus to the action rules, forming an action representation, and executing the action. Hypothetically, as the task involved no spatial orientation, no bias signal would be sent to the bottom-up attention reorienting system. The effective connectivity analysis also showed a reciprocal connection between the MFC (the core substrate of the frontoinsular network) and vermis VI. The task-related effective connectivity analysis revealed that the right MFC reinforced the activation of vermis VI and that vermis VI augmented the activation of the right MFC. These results reveal that higher MFC activation, lower vermis VI activation, and increased positive influence of the MFC on vermis VI are all associated with faster (smaller) CTI. Higher medial frontal activation induced stronger influence on vermis VI. Stronger synchronization with vermis VI thus reduced the workload of vermis VI (reduced activation), which in turn reduced the workload by speeding up the subprocesses. The interacting connections of vermis VI to the medial frontal region could thus reflect a control-automatic interaction between the two regions.

Notably, increased negative influence of vermis VI on the right SFJ (also referred to as the frontal eye field) also facilitated faster processing speed (smaller PTI) in this study. The SFJ is known to be a core substrate for the top-down orientation of attention (dorsal attention network, Corbetta and Shulman, 2002). The right SFJ, in particular, has been activated across various sensory modalities in a simple vigilant task (Langner et al., 2011) and has maintained the spatial localization of visual and auditory cues, even for cues outside of the visual field (Tark & Curtis, 2009). Therefore, the SFJ contributes to not only the visual but also the supra-modal orientation of attention. Since the finding was related to PTI but not CTI, and SFJ encoded the representation of the stimulus, it is assumed that the process was more associated with the translation of sensory information to attention system but not the rule-based decision process. The association between faster speed and increased negative influence indicated more inhibitory modulation from the vermis VI to SFJ facilitated faster sensory representation to an abstract representation of the stimulus.

Increased positive influence from Right AIP to vermis VII also facilitated faster PTI. Right AIP is a component in the dorsal attention network. It formed abstract representations of numerical magnitude regardless of the presentation of the stimulus (number of dots, Arabic number, English word, Roman numeric system) (Ansari, 2007) and representations of objects regardless of perceived modality (visual and tactile) (Grefkes, Weiss, Zilles, & Fink, 2002). Therefore, anterior IPS demonstrated symbolic and amodal representation of the transformed stimulus. On the other hand, recent brain stimulation (Esterman et al., 2017) and resting state connectivity studies (Habas:2009bj; Buckner et al., 2011) showed that vermis VII is a cerebellar node of the dorsal attention network. In particular, stimulation on vermis VII improved attention and the reaction time of a continuous performance task (Esterman et al., 2017). The causal influence from right AIP to vermis VII is hence interpreted as a cerebro-cerebellar modulation.

Increased positive influence from right MFC to vermis VI facilitated faster decision speed. MFC and Vermis VI has been found to be functionally connected to the cingulo-opercular network (Dosenbach:2006ij; Habas:2009bj; Buckner et al., 2011). Cingulo-opercular network is considered to facilitate task-set maintenance, and cerebellum acts as an internal model for the corresponding cortical region, which operates in a fast, effortless and automatic, but less flexible copy of the same mental processes in the cortex (Ito:2008bw; Ramnani, 2014). Hence, the positive influence is regarded as stronger communication of effortful task-set control to the automatic counterparts. Interestingly, fast decision speed was related to both enhanced MFC→CV6 connectivity and enhanced MFC and reduced CV6 activations. It is speculated that more effortful control (MFC) and less automatic control (vermis VI) were both associated with faster cognitive processes and it stronger communication reduced the engagement of automatic control.

The decreased positive influence of the right SFJ on the left AIP facilitated faster decision speed (CTI) in this study. The SFJ has been associated with spatial representation, and the left AIP, different from right AIP, has been related to goal representation (Hamilton & Grafton, 2006; Rice, Tunik, & Grafton, 2006). Rice and colleagues (Rice et al., 2006) applied transcranial magnetic stimulation to the anterior, middle, and caudal intraparietal sulcus, finding that stimulation in the anterior area, but not the middle or caudal areas, disrupted the execution and online adjustments of motor behavior. Rice and colleagues thus asserted that the connection of the right SFJ to the left intraparietal sulcus plays a role in translating spatial representations to action representations. The association between decreased fronto-to-parietal influence reflected that the selection of target action schema from the action set required less incoming information. It is postulated that the strength of task-set maintenance facilitated top-down attention processes, possibly by enhancing the stimulus set in SFJ and action set in AIP. First, the stronger stimulus set in SFJ speeded up the accumulation of evidence from sensory processes and hence the formation of representation of the target stimulus. The information conveyed from SFJ to AIP then consisted less noise and converged at a faster rate. Second, the action set in the intraparietal sulcus was more vivid so that the decision threshold for action schema was reached at a shorter time. Therefore, Further studies have to be conducted to examine the interplay of task-set control and top-down attention control for the facilitation of processing speed.

Conclusion

The findings of this study indicate that processing speed, decision speed and non-decision speed were influenced by facilitative and inhibitory processes that are mediated by neural substrates in the fronto-parieto-cerebellar network. This study's simple discrimination task enabled the differentiation of cognitive and non-decision processing speed. The use of both audial and visual stimuli further reduced the bias of the results through task specificity. The speed-related activation of and causal connectivities between the MFC and vermis VI/VII suggested that cognitive control played an important role in engaging the appropriate functional module in performing the action. Therefore, the strength of activations and connections were associated with differentiable components of processing speed. These findings further reveal the contributions of the cerebellum in modulating the controlled and automatic interactions of a task set related to cognitive control in processing speed.

Chapter 7 Neurophysiological Correlates of Processing Speed in Aging Population

Effective connectivity path estimation

The timeseries of the 13 selected ROIs were extracted from the older participant's 's anatomical space and input to the 1dGC.R script from AFNI to estimate path coefficients for each experimental condition. The extracted timeseries were analyzed for their stationarity using both KPSS and ADF tests and determined to use 1-TR of lagging using the AIC. Results for first level path analysis for each of the four experimental conditions and all twenty older participants were subjected to group analysis using 1dGC.R script. Both path coefficients and p-values were entered into 1dGC.R in group analysis mode. After removing 13 self-connecting paths out of the 169 possible pairwise connections, 26 effective connectivity paths retained for $p<0.0001$, and they were entered to the lasso regression model for further analysis for the older group (Table 7-1 and Figure 7-1).

Table 7-1 Path coefficients of effective connectivity in the older group

	CV6	**CV7**	**CV8**	**LSCEF**	**L6a**	**LAVI**	**LAIP**	**LLIPv**	**RSCEF**	**R6a**	**RAVI**	**RAIP**	**RLIPv**
CV6		-0.003	0.002	-0.062	-0.071	-0.064	**-0.069**	**-0.071**	-0.044	**-0.093**	**-0.121**	**-0.091**	**-0.106**
CV7	-0.017		-0.029	-0.024	-0.060	-0.009	-0.014	-0.028	-0.018	-0.030	0.046	-0.010	0.001
CV8	**0.145**	0.081		-0.017	0.036	0.022	0.060	0.036	0.007	0.052	0.009	0.009	0.026
LSCEF	0.156	**0.145**	0.133		**0.236**	**0.230**	**0.171**	0.097	0.043	**0.235**	**0.357**	0.064	0.051
L6a	**0.108**	0.043	0.060	0.065		-0.010	0.049	0.049	0.051	0.055	-0.029	0.054	0.071
LAVI	0.010	0.064	0.117	-0.025	-0.037		-0.032	0.007	-0.013	-0.006	-0.054	-0.004	-0.010
LAIP	0.104	0.016	-0.068	0.043	0.046	0.003		0.020	0.009	-0.022	-0.013	-0.031	-0.024
LLIPv	0.109	0.075	0.036	0.038	0.001	0.025	0.035		-0.007	-0.024	0.046	-0.003	-0.034
RSCEF	0.119	0.054	0.091	0.037	0.122	0.014	0.009	0.025		0.062	0.009	0.005	-0.018
R6a	0.032	-0.018	0.020	**0.156**	0.069	0.049	0.069	**0.098**	**0.100**		0.075	**0.137**	**0.165**
RAVI	-0.009	0.024	0.046	-0.009	**0.073**	-0.028	-0.017	0.030	0.008	0.049		0.059	0.051
RAIP	0.120	0.049	0.014	0.101	0.045	**0.116**	0.059	0.029	0.090	**0.183**	**0.214**		**0.235**
RLIPv	0.066	0.106	**0.141**	**-0.148**	-0.146	-0.018	0.007	-0.093	-0.121	-0.102	-0.009	-0.037	

Note: the table read from column to row. For example, index of the path from L6a to CV6 is the fifth row of the first column.

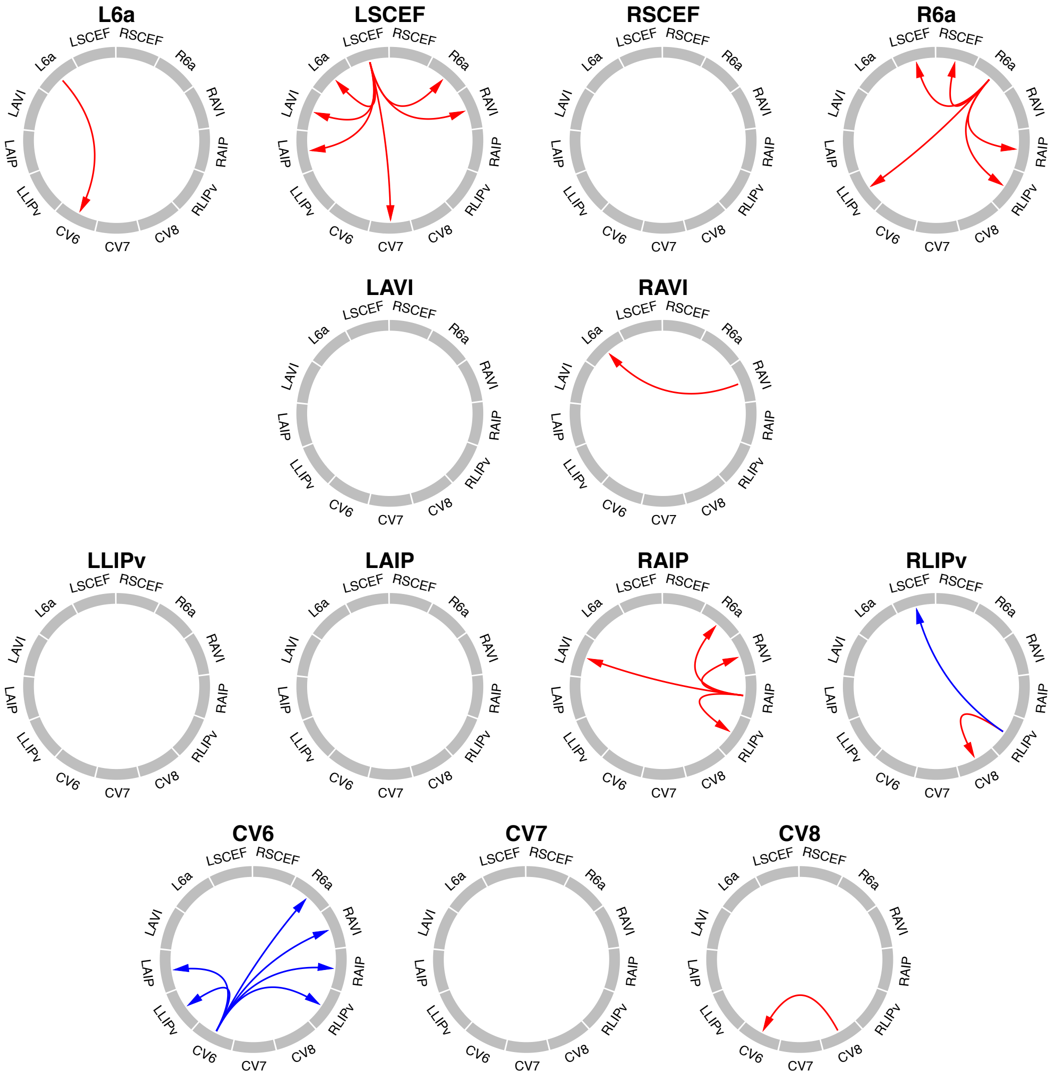

Figure 7-1 Diagram for the effective connectivity in the older group.

Note: Each diagram was labelled with the source of the causal influence. Blue arrow: negative influence, higher (or lower) activation in the source region Granger caused a lower (or higher) activation in the destination region. Red arrow: positive causal influence, higher (or lower) activation in the source region Granger caused a higher (or lower) activations in the destination region.

Speed-related activations analysis

Parameter estimates of the four experimental conditions for the thirteen selected ROIs were entered into separate linear mixed linear lasso regression model for variable selection on the three speed indices processing time index (PTI), sensorimotor time index (STI) and cognitive time index (CTI). The final model for prediction of PTI in the older group was significant ($\chi^2(2)=30.981$, $p<0.0001$, $R^2=0.2532$). Activation of the left posterior intraparietal (LLIPv, $f^2=0.57234$, $\beta=0.61162$, $p<0.001$), and the right anterior intraparietal (RAIP, $f^2=0.41543$, $\beta=-0.44151$, $p<0.001$) were significant predictors. The final model for prediction of STI was significant ($\chi^2(3)=38.753$, $p<0.0001$, $R^2=0.3874$). All predictors were significant, and included left posterior intraparietal (LLIPv, $f^2=0.75296$, $\beta=0.74568$, $p<0.001$), right medial frontal cortex (RSCEF, $f^2=0.29075$, $\beta=-0.33631$, $p=0.01$), and right anterior intraparietal (RAIP, $f^2=0.28004$, $\beta=-0.33867$, $p=0.014$). The final model for prediction of CTI was significant ($\chi^2(5)=20.046$, $p=0.0012$, $R^2=0.2106$). The model contained four significant predictors, including cerebellar vermis VII (CV7, $f^2=0.31768$, $\beta=0.46415$, $p=0.006$), right anterior intraparietal (RAIP, $f^2=0.28442$, $\beta=-0.34829$, $p=0.013$), left superior frontal junction (L6a, $f^2=0.26912$, $\beta=0.35421$, $p=0.018$), and cerebellar vermis VIII (CV8, $f^2=0.23603$, $\beta=-0.29399$, $p=0.037$), and one non-significant predictor cerebellar vermis VI (CV6, $f^2=0$, $\beta=-0.00404$, $p=0.98$).

Speed-related connectivity analysis

Estimated path coefficients for the 26 selected paths were input to three separate linear mixed effect lasso regressions for variable selection in the older group (Table 7-2 and Figure 7-2). The final model to predict PTI was significant ($\chi^2(3)=26.368$, $p<0.0001$, $R^2=0.2146$). The three included paths were left medial frontal to left superior frontal junction (LSCEF to L6a, $f^2=0.35626$, $\beta=0.32298$, $p<0.001$), left medial frontal to cerebellar vermis VII (LSCEF to CV7, $f^2=0.25824$, $\beta=-0.23295$, $p=0.009$), and right superior frontal to right anterior intraparietal (R6a to RAIP, $f^2=0.25339$, $\beta=0.23462$, $p=0.009$). The final model to predict STI was significant ($\chi^2(2)=13.396$, $p=0.0012$, $R^2=0.1509$). The two significant paths were right superior frontal to right medial frontal cortex (R6a to RSCEF, $f^2=0.36808$, $\beta=0.34488$, $p=0.002$) and left medial frontal cortex to vermis VII (LSCEF to CV7, $f^2=0.23509$, $\beta=-0.22244$, $p=0.038$). The final model predicting CTI was significant ($\chi^2(1)=14.289$, $p=0.0002$, $R^2=0.1618$) and it involved only one significant path left medial frontal cortex to left superior frontal (LSCEF to L6a, $f^2=0.43941$, $\beta=0.40444$, $p<0.001$).

Table 7-2 Best predictors selected by lasso regression on three time-indices in the older group

Model / Selected Variable	f^2	β	se	lwr	upr	p
Older group: Predict Processing Time Index with Activations						
Left Posterior Intraparietal (LLIPv)	0.572	0.612	0.103	0.403	0.813	<0.001***
Right Anterior Intraparietal (RAIP)	0.415	-0.442	0.101	-0.644	-0.251	<0.001***
Model summary: $\chi^2(2)=30.981$, $p<0.0001$, $R^2=0.2532$						
Older group: Predict Sensorimotor Time Index with Activations						
Left Posterior Intraparietal (LLIPv)	0.753	0.746	0.110	0.522	0.949	<0.001***
Right Medial Frontal Cortex (RSCEF)	0.291	-0.336	0.128	-0.573	-0.072	0.01*
Right Anterior Intraparietal (RAIP)	0.280	-0.339	0.134	-0.583	-0.100	0.014*
Model summary: $\chi^2(3)=38.753$, $p<0.0001$, $R^2=0.3874$						
Older group: Predict Cognitive Time Index with Activations						
Cerebellar Vermis VII (CV7)	0.318	0.464	0.164	0.131	0.776	0.006**
Right Anterior Intraparietal (RAIP)	0.284	-0.348	0.137	-0.613	-0.065	0.013*
Left Superior Frontal Junction (L6a)	0.269	0.354	0.147	0.062	0.643	0.018*
Cerebellar Vermis VIII (CV8)	0.236	-0.294	0.138	-0.551	0.001	0.037*
Cerebellar Vermis VI (CV6)	0.000	-0.004	0.158	-0.294	0.303	0.98
Model summary: $\chi^2(5)=20.046$,$p=0.0012$, $R^2=0.2106$						
Older group: Predict Processing Time Index with Connectivity						
Left Medial Frontal (LSCEF) to Left Superior Frontal Junction (L6a)	0.356	0.323	0.089	0.137	0.484	<0.001***
Left Medial Frontal (LSCEF) to Cerebellar Vermis VII (CV7)	0.258	-0.233	0.087	-0.407	-0.049	0.009**
Right Superior Frontal (R6a) to Right Anterior Intraparietal (RAIP)	0.253	0.235	0.088	0.056	0.427	0.009**
Model summary: $\chi^2(3)=26.368$, $p<0.0001$, $R^2=0.2146$						
Older group: Predict Sensorimotor Time Index with Connectivity						
Right Superior Frontal (R6a) to Right Medial Frontal Cortex (RSCEF)	0.368	0.345	0.105	0.141	0.581	0.002**
Left Medial Frontal Cortex (LSCEF) to Vermis VII (CV7)	0.235	-0.222	0.105	-0.426	-0.001	0.038*
Model summary: $\chi^2(2)=13.396$, $p=0.0012$, $R^2=0.1509$						
Older group: Predict Cognitive Time Index with Connectivity						
Left Medial Frontal Cortex (LSCEF) to Left Superior Frontal (L6a)	0.439	0.404	0.104	0.188	0.612	<0.001***
Model summary: $\chi^2(1)=14.289$, $p=0.0002$, $R^2=0.1618$						

Note: f^2: effect size, se: standard error, lwr/upr: lower/upper bound at 95% confidence interval, *<0.05, **<0.01, ***<0.01

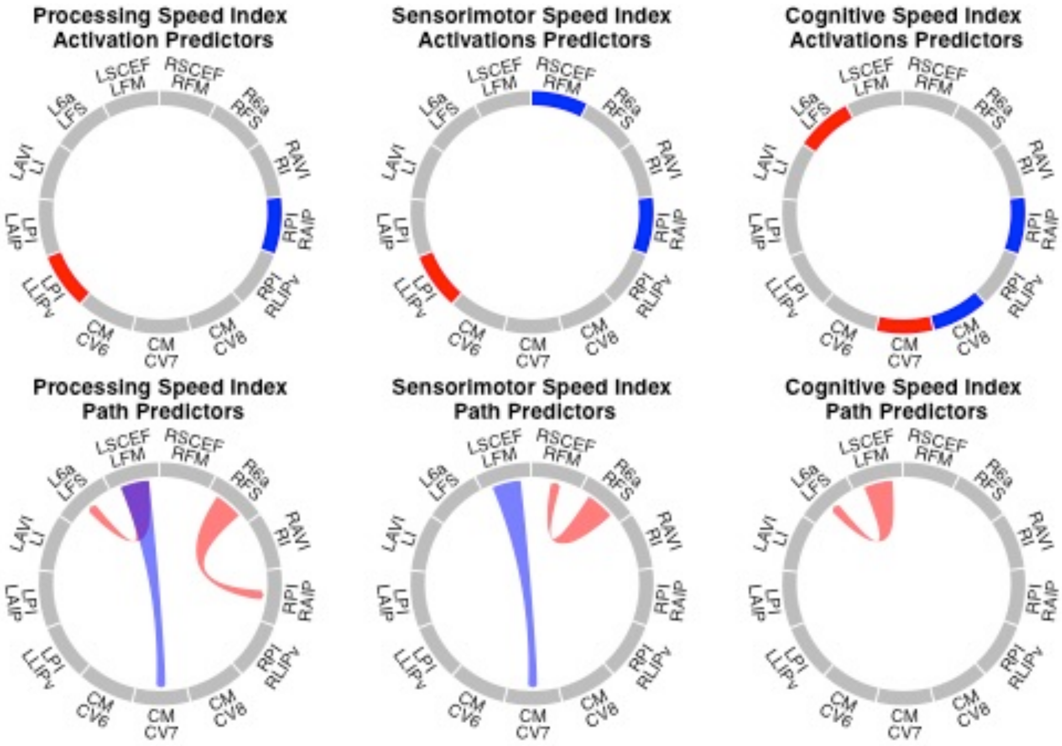

Figure 7-2 Significant activation and connectivity predictors selected by lasso regression in the older group

Note: Sections on the track represented the activation of the ROI. Blue: higher activation predicted shorter time. Red: higher activation predicted longer time. Arrows connecting different ROIs were the significant paths. Blue arrow: Decreased positive influence predicted longer time. Red arrow: Increased positive influence predicted longer time.

Discussion

The aim of this study was to explore the aging effect by comparing older adults to younger counterparts in terms of processing speed on a simple stimulus-response mapping task. The activation analysis revealed that, although the activation topography of the older and younger groups appeared to be comparable, the older participants tended to recruit more extensive frontal and parietal substrates and less extensive insular and cerebellum substrates than did the younger group. The effective connectivity analysis demonstrated that the older group had fewer interactions among brain regions than did the younger group. The bilateral MFC, intraparietal sulcus, and cerebellum had less influence on the rest of the system among older adults than among younger adults, but the bilateral SFJ exerted more causal influence. The speed-related activation analysis showed that, in the younger and older groups, increased activity in the right MFC predicted faster processing speed (smaller PTI) and faster non-decision speed (smaller STI), respectively. However, in the older group, reduced SFJ activity and enhanced intraparietal sulcus activity were associated with faster decision speed (smaller CTI), which was not found in the younger group. Vermis VII activation was found to be related to decision speed in both groups, but higher activation was associated with higher speed in the younger group and with lower speed in the older group. The speed-related effective connectivity analysis identified two lateralized frontal-to-frontal pathways in the older group—reduced left-MFC-to-left-SFJ influence (i.e., reduced positive influence predicted both faster processing and decision speed) and reduced right-SFJ-to-right-MFC influence (i.e., reduced positive influence predicted faster non-decision speed)—neither of which was found in the younger group. The increased medial frontal-to-vermis VII pathway in the older group was associated with faster processing speed and non-decision speed, but the reverse relationship occurred in the younger group.

Only one similar speed-brain correlation was found in both the younger and older groups: Higher right MFC activation predicted faster processing speed in the younger group and non-decision speed in the older group, both of which were interpreted as non-decision. The MFC was the primary substrate for implementing a stable task-set (Dosenbach et al., 2006) and to support vigilance (Langner & Eickhoff, 2013). However, the effective connectivities that interacted with the MFC differed considerably between the two groups. First, reduced positive influence of the right SFJ on the MFC was related to faster non-decision speed in the older group. These results suggest that, among the older participants who showed slower non-decision speed, the cognitive-control processes relied on input from the attention system. One possible explanation is that the older group adopted a reactive control strategy due to a decline in the functions of the cognitive-control system (Paxton, Barch, Racine, & Braver, 2008). Paxton and colleagues (2008) found that, in the younger group, the cognitive-control regions—MFC in particular—demonstrated more sustained activations, as compared to a more transient pattern among the older participants. Therefore, Paxton and colleagues postulated that the cognitive-control function remained more intact in those older participants who had relatively fast non-decision speed.

In the younger group, vermis VII was postulated to support adaptive control, as it encoded rules (Balsters et al., 2012) and pertained to the frontoparietal control network (Buckner et al., 2011; Habas et al., 2009); in addition, higher activation of this area was associated with faster decision speed (smaller CTI). In the older group, lower vermis VII, higher vermis VIII, and higher right anterior intraparietal activations all predicted faster decision speed. Lobule VIII of the cerebellum is known for its participation in sensorimotor function (Stoodley & Schmahmann, 2010). In this study, intrinsic connectivity analysis revealed that vermis VIII functionally is coupled with the sensorimotor network, which also involves the anterior intraparietal sulcus (Buckner et al., 2011; Yeo et al., 2011). The result suggests that the older group, ironically, recruits the sensorimotor system in order to perform a simple cognitive task.

In addition, this result indicates that the bilateral SFJ and intraparietal sulcus were involved in predicting at least one of the three speed indices. The SFJ and intraparietal sulcus form the dorsal attention network (Corbetta et al., 2008; Corbetta & Shulman, 2002), which performs a top-down attention-orientation function. The dorsal attention network remains intact relative to the frontoparietal control network (Grady, Sarraf, Saverino, & Campbell, 2016). A meta-analysis (H.-J. Li et al., 2015a) surveyed a hundred task-based functional MRI studies to compare the differences in activations among younger and older adults. Li and colleagues (2015a) found that, among older adults who were performing executive control tasks, the ventral attention network was hypo-activated, and the dorsal attention network was hyper-activated. Li and colleagues also asserted that older adults recruited the dorsal attention network to compensate for the functional loss of the ventral attention network, and this was associated with bottom-up attentional functioning. Older adults may thus require a higher degree of attentional control than younger adults when performing a task.

In this study, faster decision speed (smaller CTI) was associated with reduced left SFJ activity, increased right anterior intraparietal sulcus activity, and reduced positive influence of the left MFC on the left SFJ. For the younger group, it was postulated that decision speed involved the translation process in both rule and action representations (right superior frontal to left anterior intraparietal connectivity), as mentioned in Chapter 6. For the older group, the lower activation of the left SFJ and the reduced positive influence of the MFC on the left SFJ were each associated with faster decision speed. As these regions are contralateral to the translation pathway, this result is consistent with the delateralization model (Cabeza, 2002), which described a general pattern that the lateralized activation of a particular task in the younger group becomes less lateralized and has a more symmetric activation pattern with age. Although this phenomenon explains the differences between young and old, it also explains how relatively youthful older adults demonstrate less symmetric patterns (Eyler, Sherzai, Kaup, & Jeste, 2011). These results suggest that more efficient people recruit less of the left SFJ to compensate for the formation of representation.

Conclusion

This study’s results are consistent with those of previous studies, which postulated that the cognitive control and automatic processes influence processing speed (Motes et al., 2011; Rypma et al., 2006). Using a set of simple stimulus-response mapping tasks and dividing the processing speed into decision and non-decision components, this study further refined the contributions of various neural substrates. The results indicate that, instead of adaptive control in the dorsal PFC (Motes et al., 2011; Rypma et al., 2006), stable task-set control in the MFC, automaticity in the cerebellar vermis, and compensatory mechanisms in the left SFJ influence processing speed in older adults.

Chapter 8 General Discussion

Cerebello-frontoparietal Network

The cerebello-frontoparietal network can be observed in both younger and older groups. It is contended that the cerebello-frontoparietal network suggested by the current result is valid. First, recent effective connectivity studies has showed cerebellum issue causal influence to frontoparietal substrates in biological motion (Sokolov et al., 2018), verbal working memory (Sobczak-Edmans et al., 2019) and verbal learning task (Cabeza, McIntosh, Tulving, Nyberg, & Grady, 1997). In Dosenbach's study (2008) several cerebellar nodes interpose those network. In the current study, we found the vermis node was connected to both cinguloopercular and dorsal attention network. It is likely that cerebellar also facilitates communication among different functional networks. However, this require further study to clarify.

Age-related modulations of Cerebello-frontoparietal Network

CTI captured the cognitive processing time, which was specifically related to the processes which facilitated the phasic engagement of the rule-based decision process. In the young group, fronto-cerebellar and fronto-parietal influences were identified. The fronto-cerebellar influence, that is medial frontal to vermis 6 (RMFC→CV6) was found. The MFC was a core region in the cinglo-opercular network, which was associated with the maintenance of task-set, including engaging task-specific regions according to the current goal, monitoring the task performance and performance feedback. Similar to MFC, CV6 was engaged in vigilance tasks (Langner & Eickoff, 2013), which suggested that the CV6 was associated with a similar function. Also, a resting-state fMRI study reported that CV6 was intrinsically connected to the cinglo-opercular network, which further supported the functional coupling between MFC and CV6. Therefore, it is postulated that the connectivity serve as updating the internal model of task-set according to current performance, which facilitates delegation of effortful control to automatic control.

On the other hand, the right frontal eye-field to left anterior intraparietal sulcus (RSFJ→LAIP) was associated with CTI in the younger group. Since the SFJ subserved target feature selection and the LAIP was responsible for action representation, the causal influence possibly signified to the process to translate stimulus representation to goal representation, which is tentatively ascribed to the stimulus-response mapping process. The lower RSFJ→LAIP influence predicted faster speed, suggested that those fast subjects required less frontal influence to complete the mapping process. In the old group, fronto-frontal influence was observed. It is posited that LMFC→LSFJ influence is related to the refurbishment of stimulus-set representations. The SFJ served top-down attention control by maintaining the set of targets that the subject has to response to. In the old group, the stimulus-set representations could have been degraded from time to time, and the MFC monitored and reinstated the degraded contents.

The processing speed could reflect a tonic maintenance of task-set as indicated by the PTI. Tonic processes included what stimulus to focus, what rules to apply, what action to perform, before the onset of the stimulus. In the young group, cerebello-fronto and parieto-cerebellar influences are found. The vermis to frontal eye-field (CV6→RFEF) influence supported the automatic update of stimulus set, and the right anterior intraparietal to vermis VII (R AIP→CV7) implied the update of internal model for goal-related rule sets.

Interplay of Control and Automaticity for Cognitive Speed

In the young group, it appeared that the control and automaticity interact to enhance processing speed. First, stronger medial frontal facilitation to vermis 6 could be understood as monitoring of performance and update the automatic control. Stronger automatic control in vermis 6 then facilitate the maintainence of stimulus-set to attend to. This further reduce the effort for rule mapping. Further study shall be done to verify this speculation. In the old group, only fronto-frontal connectivity predicted faster cognitive speed, and it is the only significant result. In the young group, frontal eye-field recieves influence from vermis 6, but for the older subjects, frontal eye-field receives influence from medial frontal cortex. First, in the young group, the attention processes were right lateralized, and in the older group, the left hemisphere kicks in for the process. It is in general agree with the hemispheric assymetry reduction in older adult (HAROLD) model. Second, it is stipulated that the older subject required more effortful process to main stimulus set in the eye-field, as the . Furthermore, the lower influence predicted faster speed in the older group. It is suggested that slower subjects in the older group required more frontal-to-frontal compensation.

Roles of Cerebellum in Cognitive Speed

Previous study only reported vermis activation was associated with speed, but the mechanism remains unknown. The results of the current study suggested differential mechanisms for the vermis subdivisions. Vermis 6 possibly interfaces cingulo-opercular network and dorsal attention network, which is supported by previous study. Second Vermis 7 receive influence from major speed-related task regions. Therefore, vermis 7 likely to integrate information and update the internal model for the stimulus-response translation. However, Vermis 8 remain unclear, possibly associated with motor representation. Previous study suggested vermis 8 was connected to motor cortex.

Limitations

Inter-Trial Interval

In this study, the results based on simple cognitive control tasks (i.e. modified Arrow Test) on the contributions of the medial frontal cortex to cognitive processing speed were found similar to those reported using various paradigms, such as digit-symbol task (Forn, Ripollés, et al., 2013a), stop-signal task (C. S. R. Li, 2006), response inhibition tasks (Wager et al., 2005) and Rapid Visual Information Processing Task Zero (Hilti et al., 2013). The similarities in the results are somewhat counter-intuitive as the tasks cited are more complex in nature than the tasks used in this study. A close look at the design of the cited tasks revealed that all of them employed short inter-trials or inter-stimulus intervals. As the activations of the medial frontal cortex (MFC) has been reported to be responsive to trials when completed under an explicit time pressure (Forstmann et al., 2008), it is plausible that the MFC results associated with the cited tasks could have confounded by their short inter-trials or inter-stimulus intervals. Further study should examine the robustness of the role of MFC in cognitive processing speed by replicating the study using shorter and longer inter-trial interval designs.

One observation made in the older participants is that a good proportion of them did not meet the performance threshold set for the experimental tasks. This resulted in relatively small number of older participants entered into the analyses, and compared less favorable with the younger participants. The low performance among the older participants could have been attributed by the relatively short inter-trial intervals adopted in the tasks. Similarly, this could have confounded the results and future study should adjust the inter-trial intervals so that similar difficult level of the tasks can be comparable between the younger and older groups.

Potential Cognitive Control Involvement in the Control Task

Completion of the simple cognitive task of this study involved input, process and output. The control task, namely the reaction time task, was intended to capture the time spent on encoding of the visual and audial stimuli (sensory input) and making responses by pressing on a key (motor output). The “process” component of the simple cognitive task can then be partial out by removing the “input” and “output” components. The concept of generating the three time indices in this study—cognitive (CTI), sensorimotor (STI), and processing (PTI)—were based on the assumption that the reaction times of the simple cognitive task were to be dissociated into the sensorimotor and cognitive components with the contrast using the reaction times of the control task. Our result showed that in the younger group, activations of the MFC predicted PTI, but not STI and CTI. The results suggest that the activations of the MFC were not unique to the cognitive processing speed but also in the sensorimotor-related processing speed. Recent studies postulated that a top-down cognitive control component, namely task-set maintenance, could modulate the entire task (Dosenbach et al., 2006, Figure 8-1). It is plausible that the control task used in this study could have involved the task-set maintenance. On the same token, the control task, a simple reaction time, could have involved a certain extent of cognitive control. Future study is to extend the behavioral measures to quantify latencies of the encoding process (sensory input) and the motor generation separately using electroencephalography and electromyogram.

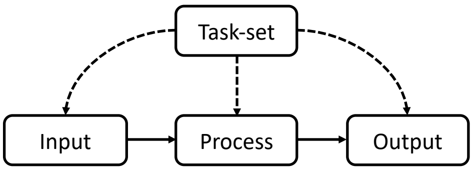

Figure 8-1 Task-set maintenance modulates input, process and output stages

The extent which the older participants would have recruited compensatory mechanisms in the experimental tasks is worth to be further explored. The results indicated that in the older group the activations of the MFC were associated with STI but not PTI and CTI. They suggest that the MFC would modulate the sensorimotor processes in the older group. Previous study reported even in very simple tasks such as those employed in this study, the task representation was found to activate the fronto-insular task-set control network (Dosenbach et al., 2006). Another study also demonstrated the sustained activations of the fronto-insular network throughout a block of trials, despite more transient patterns were shown in the (Paxton et al., 2008). Future study is to consider using a time-resolved brain imaging method to examine the time course of activations of the MFC and fronto-insular network to further validate the proposition made on its involvement in cognitive processing speed.

Statistical Concerns

Due to the small sample size and hence the effect size, limited number of ROIs were entered when developing the effective connectivity paths was limited. As a result, the ROIs related to the default mode network were not included in the current study despite the network was reported have influence on task performance in both younger (Weissman, Roberts, Visscher, & Woldorff, 2006) and older (Sambataro et al., 2010) adults. The default mode network was also found to interact with the control network causing a decay in the performance on tasks (Sridharan, Levitin, & Menon, 2008). This is a limitation of the results of this study and future study is to have a large sample size for testing more ROIs for the model of cognitive processing speed.

REFERENCES

Abram, S. V., Helwig, N. E., Moodie, C. A., DeYoung, C. G., MacDonald, A. W. I., & Waller, N. G. (2016). Bootstrap Enhanced Penalized Regression for Variable Selection with Neuroimaging Data. *Frontiers in Neuroscience*, *10*(75), 879. http://doi.org/10.3389/fnins.2016.00344

Akbar, N., Banwell, B., Sled, J. G., Binns, M. A., Doesburg, S. M., Rypma, B., et al. (2016). Brain activation patterns and cognitive processing speed in patients with pediatric-onset multiple sclerosis. *Journal of Clinical and Experimental Neuropsychology*, *38*(4), 393–403. http://doi.org/10.1080/13803395.2015.1119255

Albinet, C. T., Boucard, G., Bouquet, C. A., & Audiffren, M. (2012). Processing speed and executive functions in cognitive aging: how to disentangle their mutual relationship? *Brain and Cognition*, *79*(1), 1–11. http://doi.org/10.1016/j.bandc.2012.02.001

Ansari, D. (2007). Does the Parietal Cortex Distinguish between "10," 'Ten,' and Ten Dots? *Neuron*, *53*(2), 165–167. http://doi.org/10.1016/j.neuron.2007.01.001

Argyropoulos, G. P., Kimiskidis, V. K., & Papagiannopoulos, S. (2011). θ-burst stimulation of the right neocerebellar vermis selectively disrupts the practice-induced acceleration of lexical decisions. *Behavioral Neuroscience*, *125*(5), 724–734. http://doi.org/10.1037/a0025134

Ashburner, J., & Friston, K. J. (2000). Voxel-based morphometry--the methods. *NeuroImage*, *11*(6 Pt 1), 805–821. http://doi.org/10.1006/nimg.2000.0582

Avants, B. B., Epstein, C. L., Grossman, M., & Gee, J. C. (2008). Symmetric diffeomorphic image registration with cross-correlation: evaluating automated labeling of elderly and neurodegenerative brain. *Medical Image Analysis*, *12*(1), 26–41. http://doi.org/10.1016/j.media.2007.06.004

Avants, B. B., Tustison, N. J., Stauffer, M., Song, G., Wu, B., & Gee, J. C. (2014). The Insight ToolKit image registration framework. *Frontiers in Neuroinformatics*, *8*(52), 773. http://doi.org/10.3389/fninf.2014.00044

Balsters, J. H., Whelan, C. D., Robertson, I. H., & Ramnani, N. (2012). Cerebellum and Cognition: Evidence for the Encoding of Higher Order Rules. *Cerebral Cortex*, *23*(6), 1433–1443. http://doi.org/10.1093/cercor/bhs127

Barber, A. D., & Carter, C. S. (2004). Cognitive Control Involved in Overcoming Prepotent Response Tendencies and Switching Between Tasks. *Cerebral Cortex*, *15*(7), 899–912. http://doi.org/10.1093/cercor/bhh189

Barber, A. D., Pekar, J. J., & Mostofsky, S. H. (2016). Reaction time-related activity reflecting periodic, task-specific cognitive control. *Behavioural Brain Research*, *296*, 100–108. http://doi.org/10.1016/j.bbr.2015.08.020

Barch, D. M., & Ceaser, A. (2012). Cognition in schizophrenia: core psychological and neural mechanisms. *Trends in Cognitive Sciences*, *16*(1), 27–34. http://doi.org/10.1016/j.tics.2011.11.015

Baudouin, A., Clarys, D., Vanneste, S., & Isingrini, M. (2009). Executive functioning and processing speed in age-related differences in memory:

contribution of a coding task. *Brain and Cognition*, *71*(3), 240–245. http://doi.org/10.1016/j.bandc.2009.08.007

Bernard, J. A., & Seidler, R. D. (2013). Relationships between regional cerebellar volume and sensorimotor and cognitive function in young and older adults. *Cerebellum (London, England)*, *12*(5), 721–737. http://doi.org/10.1007/s12311-013-0481-z

Bernard, J. A., Leopold, D. R., Calhoun, V. D., & Mittal, V. A. (2015). Regional cerebellar volume and cognitive function from adolescence to late middle age. *Human Brain Mapping*, *36*(3), 1102–1120. http://doi.org/10.1002/hbm.22690

Bezdicek, O., Stepankova, H., Martinec Novakova, L., & Kopecek, M. (2016). Toward the processing speed theory of activities of daily living in healthy aging: normative data of the Functional Activities Questionnaire. *Aging Clinical and Experimental Research*, *28*(2), 239–247. http://doi.org/10.1007/s40520-015-0413-5

Bielak, A. A. M., Hughes, T. F., Small, B. J., & Dixon, R. A. (2007). It's Never Too Late to Engage in Lifestyle Activities: Significant Concurrent but not Change Relationships Between Lifestyle Activities and Cognitive Speed. *The Journals of Gerontology: Series B*, *62*(6), P331–P339. http://doi.org/10.1093/geronb/62.6.P331

Biswal, B. B., Eldreth, D. A., Motes, M. A., & Rypma, B. (2010). Task-dependent individual differences in prefrontal connectivity. *Cerebral Cortex*, *20*(9), 2188–2197. http://doi.org/10.1093/cercor/bhp284

Brissenden, J. A., Tobyne, S. M., Osher, D. E., Levin, E. J., Halko, M. A., & Somers, D. C. (2018). Topographic Cortico-cerebellar Networks Revealed by Visual Attention and Working Memory. *Current Biology : CB*, *28*(21), 3364–3372.e5. http://doi.org/10.1016/j.cub.2018.08.059

Buckner, R. L., Krienen, F. M., Castellanos, A., Diaz, J. C., & Yeo, B. T. T. (2011). The organization of the human cerebellum estimated by intrinsic functional connectivity. *Journal of Neurophysiology*, *106*(5), 2322–2345. http://doi.org/10.1152/jn.00339.2011

Bunea, F., She, Y., Ombao, H., Gongvatana, A., Devlin, K., & Cohen, R. (2011). Penalized least squares regression methods and applications to neuroimaging. *NeuroImage*, *55*(4), 1519–1527. http://doi.org/10.1016/j.neuroimage.2010.12.028

Cabeza, R. E. (2002). Hemispheric asymmetry reduction in older adults: The HAROLD model. *Psychology and Aging*, *17*(1), 85–100. http://doi.org/10.1037//0882-7974.17.1.85

Cabeza, R. E., McIntosh, A. R., Tulving, E., Nyberg, L., & Grady, C. L. (1997). Age-related differences in effective neural connectivity during encoding and recall. *Neuroreport*, *8*(16), 3479–3483. http://doi.org/10.1097/00001756-199711100-00013

Calhoun, S. L., & Mayes, S. D. (2005). Processing speed in children with clinical disorders. *Psychology in the Schools*, *42*(4), 333–343. http://doi.org/10.1002/pits.20067

Callu, D., Lopez, J., & Massioui, El, N. (2013). Cerebellar deep nuclei involvement in cognitive adaptation and automaticity. *Learning & Memory (Cold Spring Harbor, N.Y.)*, *20*(7), 344–347. http://doi.org/10.1101/lm.030536.113

Callu, D., Puget, S., Faure, A., Guegan, M., & Massioui, El, N. (2007). Habit learning dissociation in rats with lesions to the vermis and the interpositus of the cerebellum. *Neurobiology of Disease*, *27*(2), 228–237. http://doi.org/10.1016/j.nbd.2007.04.007

Carlozzi, N. E., Beaumont, J. L., Tulsky, D. S., & Gershon, R. C. (2015). The NIH Toolbox Pattern Comparison Processing Speed Test: Normative Data. *Archives of Clinical Neuropsychology*, *30*(5), 359–368. http://doi.org/10.1093/arclin/acv031

Carp, J., Fitzgerald, K. D., Taylor, S. F., & Weissman, D. H. (2012). Removing the effect of response time on brain activity reveals developmental differences in conflict processing in the posterior medial prefrontal cortex. *NeuroImage*, *59*(1), 853–860. http://doi.org/10.1016/j.neuroimage.2011.07.064

Carroll, J. B. (1993). *Human cognitive abilities: A survey of factor-analytic studies*. Cambridge, England: Cambridge University Press.

Cepeda, N. J., Blackwell, K. A., & Munakata, Y. (2013). Speed isn't everything: complex processing speed measures mask individual differences and developmental changes in executive control. *Developmental Science*, *16*(2), 269–286. http://doi.org/10.1111/desc.12024

Chen, G., Glen, D. R., Saad, Z. S., Hamilton, J. P., Thomason, M. E., Gotlib, I. H., & Cox, R. W. (2011). Vector autoregression, structural equation modeling, and their synthesis in neuroimaging data analysis. *Computers in Biology and Medicine*, *41*(12), 1142–1155. http://doi.org/10.1016/j.compbiomed.2011.09.004

Chiaravalloti, N. D., Christodoulou, C., Demaree, H. A., & DeLuca, J. (2003). Differentiating simple versus complex processing speed: influence on new learning and memory performance. *Journal of Clinical and Experimental Neuropsychology*, *25*(4), 489–501. http://doi.org/10.1076/jcen.25.4.489.13878

Cieslik, E. C., Zilles, K., Kurth, F., & Eickhoff, S. B. (2010). Dissociating bottom-up and top-down processes in a manual stimulus-response compatibility task. *Journal of Neurophysiology*, *104*(3), 1472–1483. http://doi.org/10.1152/jn.00261.2010

Cole, M. W., Bassett, D. S., Power, J. D., Braver, T. S., & Petersen, S. E. (2014a). Intrinsic and task-evoked network architectures of the human brain. *Neuron*, *83*(1), 238–251. http://doi.org/10.1016/j.neuron.2014.05.014

Cole, M. W., Repovs, G., & Anticevic, A. (2014b). The frontoparietal control system: a central role in mental health., *20*(6), 652–664. http://doi.org/10.1177/1073858414525995

Corbetta, M., & Shulman, G. L. (2002). Control of goal-directed and stimulus-driven attention in the brain. *Nature Reviews Neuroscience*, *3*(3), 201–215. http://doi.org/10.1038/nrn755

Corbetta, M., Patel, G., & Shulman, G. L. (2008). The reorienting system of the human brain: from environment to theory of mind. *Neuron*, *58*(3), 306–324. http://doi.org/10.1016/j.neuron.2008.04.017

Costa, S. L., Genova, H. M., DeLuca, J., & Chiaravalloti, N. D. (2016). Information processing speed in multiple sclerosis: Past, present, and future. *Multiple Sclerosis (Houndmills, Basingstoke, England)*. http://doi.org/10.1177/1352458516645869

Coyle, T. R., Pillow, D. R., Snyder, A. C., & Kochunov, P. (2011). Processing Speed Mediates the Development of General Intelligence (g) in Adolescence:. *Psychological Science*, *22*(10), 1265–1269. http://doi.org/10.1177/0956797611418243

Danthiir, V., Wilhelm, O., Schulze, R., & Roberts, R. D. (2005). Factor structure and validity of paper-and-pencil measures of mental speed: Evidence for a higher-order model? *Intelligence*, *33*(5), 491–514. http://doi.org/10.1016/j.intell.2005.03.003

Dawson, M. R. W. (1988). Fitting the ex-Gaussian equation to reaction time distributions. *Behavior Research Methods, Instruments, & Computers*, *20*(1), 54–57. http://doi.org/10.3758/BF03202603

Deary, I. J. (2001). Reaction times and intelligence differences A population-based cohort study. *Intelligence*, *29*(5), 389–399. http://doi.org/10.1016/s0160-2896(01)00062-9

Der, G., & Deary, I. J. (2003). IQ, reaction time and the differentiation hypothesis. *Intelligence*, *31*(5), 491–503. http://doi.org/10.1016/S0160-2896(02)00189-7

Desikan, R. S., Ségonne, F., Fischl, B., Quinn, B. T., Dickerson, B. C., Blacker, D., et al. (2006). An automated labeling system for subdividing the human cerebral cortex on MRI scans into gyral based regions of interest. *NeuroImage*, *31*(3), 968–980. http://doi.org/10.1016/j.neuroimage.2006.01.021

Deverett, B., Koay, S. A., Oostland, M., & Wang, S. S. H. (2018). Cerebellar involvement in an evidence-accumulation decision-making task. *eLife*, *7*, 368. http://doi.org/10.7554/eLife.36781

Dolan, C. V., van der Maas, H. L. J., & Molenaar, P. C. M. (2002). A framework for ML estimation of parameters of (mixtures of) common reaction time distributions given optional truncation or censoring. *Behavior Research Methods, Instruments, & Computers*, *34*(3), 304–323. http://doi.org/10.3758/BF03195458

Domagalik, A., Beldzik, E., Oginska, H., Marek, T., & Fafrowicz, M. (2014). Inconvenient correlation - RT-BOLD relationship for homogeneous and fast reactions. *Neuroscience*, *278*, 211–221. http://doi.org/10.1016/j.neuroscience.2014.08.012

Donders, F. C. (1969). On the speed of mental processes. *Acta Psychologica*, *30*, 412–431. http://doi.org/10.1016/0001-6918(69)90065-1

Dosenbach, N. U. F., Fair, D. A., Cohen, A. L., Schlaggar, B. L., & Petersen, S. E. (2008). A dual-networks architecture of top-down control. *Trends in Cognitive Sciences*, *12*(3), 99–105. http://doi.org/10.1016/j.tics.2008.01.001

Dosenbach, N. U. F., Fair, D. A., Miezin, F. M., Cohen, A. L., Wenger, K. K., Dosenbach, R. A. T., et al. (2007). Distinct brain networks for adaptive and stable task control in humans. *Proceedings of the National Academy of Sciences*, *104*(26), 11073–11078. http://doi.org/10.1073/pnas.0704320104

Dosenbach, N. U. F., Visscher, K. M., Palmer, E. D., Miezin, F. M., Wenger, K. K., Kang, H. C., et al. (2006). A core system for the implementation of task sets. *Neuron*, *50*(5), 799–812. http://doi.org/10.1016/j.neuron.2006.04.031

Duncan, J. (2010). The multiple-demand (MD) system of the primate brain: mental programs for intelligent behaviour. *Trends in Cognitive Sciences*, *14*(4), 172–179. http://doi.org/10.1016/j.tics.2010.01.004

E, K.-H., Chen, S.-H. A., Ho, M.-H. R., & Desmond, J. E. (2014). A meta-analysis of cerebellar contributions to higher cognition from PET and fMRI studies. *Human Brain Mapping*, *35*(2), 593–615. http://doi.org/10.1002/hbm.22194

Eckert, M. A. (2011). Slowing down: age-related neurobiological predictors of processing speed. *Frontiers in Neuroscience*, *5*, 25. http://doi.org/10.3389/fnins.2011.00025

Eckert, M. A., Keren, N. I., Roberts, D. R., Calhoun, V. D., & Harris, K. C. (2010). Age-related changes in processing speed: unique contributions of cerebellar and prefrontal cortex. *Frontiers in Human Neuroscience*, *4*, 10. http://doi.org/10.3389/neuro.09.010.2010

Esterman, M., Thai, M., Okabe, H., DeGutis, J., Saad, E., Laganiere, S. E., & Halko, M. A. (2017). Network-targeted cerebellar transcranial magnetic stimulation improves attentional control. *NeuroImage*, *156*, 190–198. http://doi.org/10.1016/j.neuroimage.2017.05.011

Eyler, L. T., Sherzai, A., Kaup, A. R., & Jeste, D. V. (2011). A review of functional brain imaging correlates of successful cognitive aging. *Biological …*, *70*(2), 115–122. http://doi.org/10.1016/j.biopsych.2010.12.032

Fan, J. (2014). An information theory account of cognitive control. *Frontiers in Human Neuroscience*, *8*(598), 680. http://doi.org/10.3389/fnhum.2014.00680

Fan, J., McCandliss, B. D., Fossella, J., Flombaum, J. I., & Posner, M. I. (2005). The activation of attentional networks. *NeuroImage*, *26*(2), 471–479. http://doi.org/10.1016/j.neuroimage.2005.02.004

Finkel, D., & Pedersen, N. L. (2010). Processing Speed and Longitudinal Trajectories of Change for Cognitive Abilities: The Swedish Adoption/Twin Study of Aging. *Aging, Neuropsychology, and Cognition*, *11*(2-3), 325–345. http://doi.org/10.1080/13825580490511152

Finkel, D., Reynolds, C. A., McArdle, J. J., & Pedersen, N. L. (2007). Age changes in processing speed as a leading indicator of cognitive aging. *Psychology and Aging*, *22*(3), 558–568. http://doi.org/10.1037/0882-7974.22.3.558

Fischl, B., & Dale, A. M. (2000). Measuring the thickness of the human cerebral cortex from magnetic resonance images. *Proceedings of the National Academy of Sciences*, *97*(20), 11050–11055. http://doi.org/10.1073/pnas.200033797

Forn, C., Belenguer, A., Belloch, V., Sanjuan, A., Parcet, M. A., & Ávila, C. (2011). Anatomical and functional differences between the Paced Auditory Serial Addition Test and the Symbol Digit Modalities Test. *Journal of Clinical and Experimental Neuropsychology*, *33*(1), 42–50. http://doi.org/10.1080/13803395.2010.481620

Forn, C., Belloch, V., Bustamante, J. C., Garbin, G., Parcet-Ibars, M. À., Sanjuan, A., et al. (2009). A symbol digit modalities test version suitable for functional MRI studies. *Neuroscience Letters*, *456*(1), 11–14. http://doi.org/10.1016/j.neulet.2009.03.081

Forn, C., Ripollés, P., Cruz-Gómez, A. J., Belenguer, A., González-Torre, J. A., & Ávila, C. (2013a). Task-load manipulation in the Symbol Digit Modalities Test: an alternative measure of information processing speed. *Brain and Cognition*, *82*(2), 152–160. http://doi.org/10.1016/j.bandc.2013.04.003

Forn, C., Rocca, M. A., Boscá, I., Casanova, B., Sanjuan, A., & Filippi, M. (2013b). Analysis of "task-positive" and “task-negative” functional networks during the performance of the Symbol Digit Modalities Test in patients at presentation with clinically isolated syndrome suggestive of multiple sclerosis. *Experimental Brain Research*, *225*(3), 399–407. http://doi.org/10.1007/s00221-012-3380-5

Forstmann, B. U., Dutilh, G., Brown, S., Neumann, J., Cramon, von, D. Y., Ridderinkhof, K. R., & Wagenmakers, E.-J. (2008). Striatum and pre-SMA facilitate decision-making under time pressure. *Proceedings of the National Academy of Sciences*, *105*(45), 17538–17542. http://doi.org/10.1073/pnas.0805903105

Fox, M. D., & Greicius, M. D. (2010). Clinical applications of resting state functional connectivity. *Frontiers in Systems Neuroscience*, *4*, 19. http://doi.org/10.3389/fnsys.2010.00019

Fox, M. D., Snyder, A. Z., Vincent, J. L., Corbetta, M., Van Essen, D. C., & Raichle, M. E. (2005). The human brain is intrinsically organized into dynamic, anticorrelated functional networks. *Proceedings of the National Academy of Sciences*, *102*(27), 9673–9678. http://doi.org/10.1073/pnas.0504136102

Fratiglioni, L., Paillard-Borg, S., & Winblad, B. (2004). An active and socially integrated lifestyle in late life might protect against dementia. *The Lancet. Neurology*, *3*(6), 343–353. http://doi.org/10.1016/S1474-4422(04)00767-7

Gazes, Y., Bowman, F. D., Razlighi, Q. R., O'Shea, D., Stern, Y., & Habeck, C. G. (2016). White matter tract covariance patterns predict age-declining cognitive abilities. *NeuroImage*, *125*, 53–60. http://doi.org/10.1016/j.neuroimage.2015.10.016

Genova, H. M., Hillary, F. G., Wylie, G., Rypma, B., & DeLuca, J. (2009). Examination of processing speed deficits in multiple sclerosis using functional magnetic resonance imaging. *Journal of the International Neuropsychological Society*, *15*(3), 383–393. http://doi.org/10.1017/S1355617709090535

Glasser, M. F., Coalson, T. S., Robinson, E. C., Hacker, C. D., Harwell, J., Yacoub, E., et al. (2016). A multi-modal parcellation of human cerebral cortex. *Nature*, *536*(7615), 171–178. http://doi.org/10.1038/nature18933

Grady, C. L., Sarraf, S., Saverino, C., & Campbell, K. (2016). Age differences in the functional interactions among the default, frontoparietal control, and dorsal attention networks. *Neurobiology of Aging*, *41*, 159–172. http://doi.org/10.1016/j.neurobiolaging.2016.02.020

Granger, C. W. J. (1969). Investigating Causal Relations by Econometric Models and Cross-spectral Methods. *Econometrica*, *37*(3), 424. http://doi.org/10.2307/1912791

Grefkes, C., Weiss, P. H., Zilles, K., & Fink, G. R. (2002). Crossmodal Processing of Object Features in Human Anterior Intraparietal Cortex. *Neuron*, *35*(1), 173–184. http://doi.org/10.1016/S0896-6273(02)00741-9

Groll, A., & Tutz, G. (2014). Variable selection for generalized linear mixed models by L 1-penalized estimation. *Statistics and Computing*, *24*(2), 137–154. http://doi.org/10.1007/s11222-012-9359-z

Habas, C., Kamdar, N., Nguyen, D., Prater, K., Beckmann, C. F., Menon, V., & Greicius, M. D. (2009). Distinct cerebellar contributions to intrinsic connectivity networks. *The Journal of Neuroscience : the Official Journal of the Society for Neuroscience*, *29*(26), 8586–8594. http://doi.org/10.1523/JNEUROSCI.1868-09.2009

Habeck, C. G., Gazes, Y., Razlighi, Q., Steffener, J., Brickman, A., Barulli, D., et al. (2016). The Reference Ability Neural Network Study: Life-time stability of reference-ability neural networks derived from task maps of young adults. *NeuroImage*, *125*, 693–704. http://doi.org/10.1016/j.neuroimage.2015.10.077

Habeck, C. G., Steffener, J., Barulli, D., Gazes, Y., Razlighi, Q., Shaked, D., et al. (2015). Making cognitive latent variables manifest: distinct neural networks for fluid reasoning and processing speed. *Journal of Cognitive Neuroscience*, *27*(6), 1249–1258. http://doi.org/10.1162/jocn_a_00778

Hale, S. (1990). A global developmental trend in cognitive processing speed. *Child Development*, *61*(3), 653–663.

Hamilton, A. F. de C., & Grafton, S. T. (2006). Goal representation in human anterior intraparietal sulcus. *The Journal of Neuroscience : the Official Journal of the Society for Neuroscience*, *26*(4), 1133–1137. http://doi.org/10.1523/JNEUROSCI.4551-05.2006

Han, L., Gill, T. M., Jones, B. L., & Allore, H. G. (2016). Cognitive Aging Trajectories and Burdens of Disability, Hospitalization and Nursing Home Admission Among Community-living Older Persons. *The Journals of Gerontology. Series a, Biological Sciences and Medical Sciences*, *71*(6), 766–771. http://doi.org/10.1093/gerona/glv159

Hastie, T., Tibshirani, R., & Friedman, J. (2008). Linear Methods for Regression. In *The Elements of Statistical Learning* (pp. 1–57). New York, NY: Springer New York. http://doi.org/10.1007/b94608_3

Herzfeld, D. J., Kojima, Y., Soetedjo, R., & Shadmehr, R. (2018). Encoding of error and learning to correct that error by the Purkinje cells of the cerebellum. *Nature Neuroscience*, *21*(5), 736–743. http://doi.org/10.1038/s41593-018-0136-y

Hillary, F. G., Genova, H. M., Medaglia, J. D., Fitzpatrick, N. M., Chiou, K. S., Wardecker, B. M., et al. (2010). The nature of processing speed deficits in traumatic brain injury: is less brain more? *Brain Imaging and Behavior*, *4*(2), 141–154. http://doi.org/10.1007/s11682-010-9094-z

Hilti, C. C., Jann, K., Heinemann, D., Federspiel, A., Dierks, T., Seifritz, E., & Cattapan-Ludewig, K. (2013). Evidence for a cognitive control network for goal-directed attention in simple sustained attention. *Brain and Cognition*, *81*(2), 193–202. http://doi.org/10.1016/j.bandc.2012.10.013

Hoerl, A. E., & Kennard, R. W. (2012). Ridge Regression: Biased Estimation for Nonorthogonal Problems. *Technometrics*, *12*(1), 55–67. http://doi.org/10.1080/00401706.1970.10488634

Hogan, M. J. (2004). The cerebellum in thought and action: a fronto-cerebellar aging hypothesis. *New Ideas in Psychology*, *22*(2), 97–125. http://doi.org/10.1016/j.newideapsych.2004.09.002

Hugdahl, K., Raichle, M. E., Mitra, A., & Specht, K. (2015). On the existence of a generalized non-specific task-dependent network. *Frontiers in Human Neuroscience*, *9*, 430. http://doi.org/10.3389/fnhum.2015.00430

Jenkinson, M., Beckmann, C. F., Behrens, T. E. J., Woolrich, M. W., & Smith, S. M. (2012). FSL. *NeuroImage*, *62*(2), 782–790. http://doi.org/10.1016/j.neuroimage.2011.09.015

Jensen, A. R. (2006). Clocking the Mind. Elsevier. http://doi.org/10.1111/j.1744-6570.2008.00111_7.x

Jensen, A. R., & Reed, T. E. (1990). Simple reaction time as a suppressor variable in the chronometric study of intelligence. *Intelligence*, *14*(4), 375–388. http://doi.org/10.1016/s0160-2896(05)80011-x

Kail, R. V., & Salthouse, T. A. (1994). Processing speed as a mental capacity. *Acta Psychologica*, *86*(2-3), 199–225. http://doi.org/10.1016/0001-6918(94)90003-5

Kansaku, K., Hanakawa, T., Wu, T., & Hallett, M. (2004). A shared neural network for simple reaction time. *NeuroImage*, *22*(2), 904–911. http://doi.org/10.1016/j.neuroimage.2004.02.006

Kelly, R. E., Alexopoulos, G. S., Wang, Z., Gunning, F. M., Murphy, C. F., Morimoto, S. S., et al. (2010). Visual inspection of independent components: defining a procedure for artifact removal from fMRI data. *Journal of*

Neuroscience Methods, *189*(2), 233–245. http://doi.org/10.1016/j.jneumeth.2010.03.028

Kelly, R. M., & Strick, P. L. (2003). Cerebellar loops with motor cortex and prefrontal cortex of a nonhuman primate. *The Journal of Neuroscience : the Official Journal of the Society for Neuroscience*, *23*(23), 8432–8444.

Kim, H. (2014). Involvement of the dorsal and ventral attention networks in oddball stimulus processing: a meta-analysis. *Human Brain Mapping*, *35*(5), 2265–2284. http://doi.org/10.1002/hbm.22326

Kim, K., Carp, J., Fitzgerald, K. D., Taylor, S. F., & Weissman, D. H. (2013). Neural congruency effects in the multi-source interference task vanish in healthy youth after controlling for conditional differences in mean RT. *PLoS ONE*, *8*(4), e60710. http://doi.org/10.1371/journal.pone.0060710

Klein, A., Andersson, J., Ardekani, B. A., Ashburner, J., Avants, B., Chiang, M.-C., et al. (2009). Evaluation of 14 nonlinear deformation algorithms applied to human brain MRI registration. *NeuroImage*, *46*(3), 786–802. http://doi.org/10.1016/j.neuroimage.2008.12.037

Kleine, J. F., Guan, Y., & Buttner, U. (2003). Discharge properties of saccade-related neurons in the primate fastigial oculomotor region. *Annals of the New York Academy of Sciences*, *1004*, 252–261. http://doi.org/10.1196/annals.1303.022

Koziol, L. F., Budding, D., Andreasen, N., D'Arrigo, S., Bulgheroni, S., Imamizu, H., et al. (2014). Consensus paper: the cerebellum's role in movement and cognition. (2nd ed., Vol. 13, pp. 151–177). Presented at the Cerebellum (London, England). http://doi.org/10.1007/s12311-013-0511-x

Lang, C. E., & Bastian, A. J. (2002). Cerebellar Damage Impairs Automaticity of a Recently Practiced Movement. *Journal of Neurophysiology*, *87*(3), 1336–1347. http://doi.org/10.1152/jn.00368.2001

Langner, R., & Eickhoff, S. B. (2013). Sustaining attention to simple tasks: a meta-analytic review of the neural mechanisms of vigilant attention. *Psychological Bulletin*, *139*(4), 870–900. http://doi.org/10.1037/a0030694

Langner, R., Kellermann, T., Eickhoff, S. B., Boers, F., Chatterjee, A., Willmes, K., & Sturm, W. (2011). Staying responsive to the world: Modality-specific and -nonspecific contributions to speeded auditory, tactile, and visual stimulus detection. *Human Brain Mapping*, *33*(2), 398–418. http://doi.org/10.1002/hbm.21220

Laukka, E. J., Lövdén, M., Kalpouzos, G., Papenberg, G., Keller, L., Graff, C., et al. (2015). Microstructural White Matter Properties Mediate the Association between APOE and Perceptual Speed in Very Old Persons without Dementia. *PLoS ONE*, *10*(8), e0134766. http://doi.org/10.1371/journal.pone.0134766

Laurin, C., Boomsma, D., & Lubke, G. (2016). The use of vector bootstrapping to improve variable selection precision in Lasso models. *Statistical Applications in Genetics and Molecular Biology*, *15*(4), 305–320. http://doi.org/10.1515/sagmb-2015-0043

Leavitt, V. M., Wylie, G., Genova, H. M., Chiaravalloti, N. D., & DeLuca, J. (2012). Altered effective connectivity during performance of an information processing speed task in multiple sclerosis. *Multiple Sclerosis (Houndmills, Basingstoke, England)*, *18*(4), 409–417. http://doi.org/10.1177/1352458511423651

Lee, T. M. C., Zhang, J. X., Chan, C. C. H., Yuen, K. S. L., Chu, L. W., Cheung, R. T. F., et al. (2006). Age-related differences in response regulation as revealed by functional MRI. *Brain Research*, *1076*(1), 171–176. http://doi.org/10.1016/j.brainres.2005.12.124

Lee, T. M. C., Zhou, W.-H., Luo, X.-J., Yuen, K. S. L., Ruan, X.-Z., & Weng, X.-C. (2005). Neural activity associated with cognitive regulation in heroin users: A fMRI study. *Neuroscience Letters*, *382*(3), 211–216. http://doi.org/10.1016/j.neulet.2005.03.053

Lee, T., Crawford, J. D., Henry, J. D., Trollor, J. N., Kochan, N. A., Wright, M. J., et al. (2012). Mediating effects of processing speed and executive functions in age-related differences in episodic memory performance: a cross-validation study. *Neuropsychology*, *26*(6), 776–784. http://doi.org/10.1037/a0030053

Li, C. S. R. (2006). Imaging Response Inhibition in a Stop-Signal Task: Neural Correlates Independent of Signal Monitoring and Post-Response Processing. *The Journal of Neuroscience : the Official Journal of the Society for Neuroscience*, *26*(1), 186–192. http://doi.org/10.1523/jneurosci.3741-05.2006

Li, H.-J., Hou, X.-H., Liu, H.-H., Yue, C.-L., Lu, G.-M., & Zuo, X.-N. (2015a). Putting age-related task activation into large-scale brain networks: A meta-analysis of 114 fMRI studies on healthy aging. *Neuroscience and Biobehavioral Reviews*, *57*, 156–174. http://doi.org/10.1016/j.neubiorev.2015.08.013

Li, Q., Wang, K., Nan, W., Zheng, Y., Wu, H., Wang, H., & Liu, X. (2015b). Electrophysiological dynamics reveal distinct processing of stimulus-stimulus and stimulus-response conflicts. *Psychophysiology*, *52*(4), 562–571. http://doi.org/10.1111/psyp.12382

Logan, G. D. (1992). Shapes of reaction-time distributions and shapes of learning curves: a test of the instance theory of automaticity. *Journal of Experimental Psychology. Learning, Memory, and Cognition*, *18*(5), 883–914.

Madden, D. J., Whiting, W. L., Provenzale, J. M., & Huettel, S. A. (2004). Age-related changes in neural activity during visual target detection measured by fMRI. *Cerebral Cortex*, *14*(2), 143–155.

McAuley, T., & White, D. A. (2011). A latent variables examination of processing speed, response inhibition, and working memory during typical development. *Journal of Experimental Child Psychology*, *108*(3), 453–468. http://doi.org/10.1016/j.jecp.2010.08.009

McNeish, D. M. (2015). Using Lasso for Predictor Selection and to Assuage Overfitting: A Method Long Overlooked in Behavioral Sciences. *Multivariate Behavioral Research*, *50*(5), 471–484. http://doi.org/10.1080/00273171.2015.1036965

Miller, T. D., Ferguson, K. J., Reid, L. M., Wardlaw, J. M., Starr, J. M., Seckl, J. R., et al. (2013). Cerebellar vermis size and cognitive ability in community-dwelling elderly men. *Cerebellum (London, England)*, *12*(1), 68–73. http://doi.org/10.1007/s12311-012-0397-z

Moroso, A., Ruet, A., Lamargue-Hamel, D., Munsch, F., Deloire, M., Coupé, P., et al. (2017). Posterior lobules of the cerebellum and information processing speed at various stages of multiple sclerosis. *Journal of Neurology, Neurosurgery & Psychiatry*, *88*(2), 146–151. http://doi.org/10.1136/jnnp-2016-313867

Motes, M. A., Biswal, B. B., & Rypma, B. (2011). Age-Dependent Relationships between Prefrontal Cortex Activation and Processing Efficiency. *Cognitive Neuroscience*, *2*(1), 1–10. http://doi.org/10.1080/17588928.2010.512974

Mottaghy, F. M., Willmes, K., Horwitz, B., Müller, H.-W., Krause, B. J., & Sturm, W. (2006). Systems level modeling of a neuronal network subserving intrinsic alertness. *NeuroImage*, *29*(1), 225–233. http://doi.org/10.1016/j.neuroimage.2005.07.034

Mulder, H., Pitchford, N. J., & Marlow, N. (2010). Processing speed and working memory underlie academic attainment in very preterm children. *Archives of Disease in Childhood - Fetal and Neonatal Edition*, *95*(4), F267–F272. http://doi.org/10.1136/adc.2009.167965

Murray, C. J. L., Barber, R. M., Foreman, K. J., Ozgoren, A. A., Abd-Allah, F., Abera, S. F., et al. (2015). Global, regional, and national disability-adjusted life years (DALYs) for 306 diseases and injuries and healthy life expectancy (HALE) for 188 countries, 1990–2013: quantifying the epidemiological transition. *Lancet (London, England)*, *386*(10009), 2145–2191. http://doi.org/10.1016/S0140-6736(15)61340-X

Nadkarni, N. K., Nunley, K. A., Aizenstein, H. J., Harris, T. B., Yaffe, K., Satterfield, S., et al. (2014). Association between cerebellar gray matter volumes, gait speed, and information-processing ability in older adults enrolled in the Health ABC study. *The Journals of Gerontology. Series a, Biological Sciences and Medical Sciences*, *69*(8), 996–1003. http://doi.org/10.1093/gerona/glt151

Nazeri, A., Chakravarty, M. M., Rajji, T. K., Felsky, D., Rotenberg, D. J., Mason, M., et al. (2015). Superficial white matter as a novel substrate of age-related cognitive decline. *Neurobiology of Aging*, *36*(6), 2094–2106. http://doi.org/10.1016/j.neurobiolaging.2015.02.022

Nichols, T., Brett, M., Andersson, J., Wager, T. D., & Poline, J.-B. (2005). Valid conjunction inference with the minimum statistic. *NeuroImage*, *25*(3), 653–660. http://doi.org/10.1016/j.neuroimage.2004.12.005

Nielsen, S., & Wilms, L. I. (2014). Cognitive aging on latent constructs for visual processing capacity: a novel structural equation modeling framework with causal assumptions based on a theory of visual attention. *Frontiers in Psychology*, *5*, 1596. http://doi.org/10.3389/fpsyg.2014.01596

Oldfield, R. C. (1971). The assessment and analysis of handedness: The Edinburgh inventory. *Neuropsychologia*, *9*(1), 97–113. http://doi.org/10.1016/0028-3932(71)90067-4

Owens, C. B., de Boer, C., Gennari, G., Broersen, R., Pel, J. J., Miller, B., et al. (2018). Early Trajectory Prediction in Elite Athletes. *Cerebellum (London, England)*, *17*(6), 766–776. http://doi.org/10.1007/s12311-018-0975-9

Owsley, C., Sloane, M., McGwin, G., & Ball, K. (2002). Timed instrumental activities of daily living tasks: relationship to cognitive function and everyday performance assessments in older adults. *Gerontology*, *48*(4), 254–265. http://doi.org/10.1159/000058360

Palmer, E. M., Horowitz, T. S., Torralba, A., & Wolfe, J. M. (2011). What are the shapes of response time distributions in visual search? *Journal of Experimental Psychology. Human Perception and Performance*, *37*(1), 58–71. http://doi.org/10.1037/a0020747

Paul, R., Grieve, S. M., Chaudary, B., Gordon, N., Lawrence, J., Cooper, N., et al. (2009). Relative contributions of the cerebellar vermis and prefrontal lobe volumes on cognitive function across the adult lifespan. *Neurobiology of Aging*, *30*(3), 457–465. http://doi.org/10.1016/j.neurobiolaging.2007.07.017

Paxton, J. L., Barch, D. M., Racine, C. A., & Braver, T. S. (2008). Cognitive control, goal maintenance, and prefrontal function in healthy aging. *Cerebral Cortex*, *18*(5), 1010–1028. http://doi.org/10.1093/cercor/bhm135

Perneczky, R., Pohl, C., Sorg, C., Hartmann, J., Komossa, K., Alexopoulos, P., et al. (2006). Complex activities of daily living in mild cognitive impairment: conceptual and diagnostic issues. *Age and Ageing*, *35*(3), 240–245. http://doi.org/10.1093/ageing/afj054

Peterburs, J., & Desmond, J. E. (2016). The role of the human cerebellum in performance monitoring. *Current Opinion in Neurobiology*, *40*, 38–44. http://doi.org/10.1016/j.conb.2016.06.011

Petersen, S. E., & Posner, M. I. (2012). The attention system of the human brain: 20 years after. *Annual Review of Neuroscience*, *35*, 73–89. http://doi.org/10.1146/annurev-neuro-062111-150525

Pischedda, D., Görgen, K., Haynes, J.-D., & Reverberi, C. (2017). Neural Representations of Hierarchical Rule Sets: the Human Control System Represents Rules Irrespective of the Hierarchical Level They Belong to. *The Journal of Neuroscience : the Official Journal of the Society for Neuroscience*. http://doi.org/10.1523/JNEUROSCI.3088-16.2017

Posner, M. I. (2005). Timing the brain: mental chronometry as a tool in neuroscience. *PLoS Biology*, *3*(2), e51. http://doi.org/10.1371/journal.pbio.0030051

Preckel, F., Wermer, C., & Spinath, F. M. (2011). The interrelationship between speeded and unspeeded divergent thinking and reasoning, and the role of mental speed. *Intelligence*, *39*(5), 378–388. http://doi.org/10.1016/j.intell.2011.06.007

Raichle, M. E., & Snyder, A. Z. (2007). A default mode of brain function: a brief history of an evolving idea. *NeuroImage*, *37*(4), 1083–90– discussion 1097–9. http://doi.org/10.1016/j.neuroimage.2007.02.041

Ramnani, N. (2014). Automatic and controlled processing in the corticocerebellar system. *Progress in Brain Research*, *210*, 255–285. http://doi.org/10.1016/B978-0-444-63356-9.00010-8

Rao, N. K., Motes, M. A., & Rypma, B. (2014). Investigating the neural bases for intra-subject cognitive efficiency changes using functional magnetic resonance imaging. *Frontiers in Human Neuroscience*, *8*(e4257), 840. http://doi.org/10.3389/fnhum.2014.00840

Ratcliff, R. (1978). A theory of memory retrieval. *Psychological Review*, *85*(2), 59–108. http://doi.org/10.1037/0033-295x.85.2.59

Rice, N. J., Tunik, E., & Grafton, S. T. (2006). The Anterior Intraparietal Sulcus Mediates Grasp Execution, Independent of Requirement to Update: New Insights from Transcranial Magnetic Stimulation. *The Journal of Neuroscience : the Official Journal of the Society for Neuroscience*, *26*(31), 8176–8182. http://doi.org/10.1523/JNEUROSCI.1641-06.2006

Rikli, R. E., & Edwards, D. J. (1991). Effects of a three-year exercise program on motor function and cognitive processing speed in older women. *Research Quarterly for Exercise and Sport*, *62*(1), 61–67. http://doi.org/10.1080/02701367.1991.10607519

Roberts, R. D., & Stankov, L. (1999). Individual differences in speed of mental processing and human cognitive abilities: Toward a taxonomic model. *Learning and Individual Differences*, *11*(1), 1–120. http://doi.org/10.1016/S1041-6080(00)80007-2

Rohde, T. E., & Thompson, L. A. (2007). Predicting academic achievement with cognitive ability. *Intelligence*, *35*(1), 83–92. http://doi.org/10.1016/j.intell.2006.05.004

Ruet, A., Hamel, D., Deloire, M. S. A., Charré-Morin, J., Saubusse, A., & Brochet, B. (2014). Information processing speed impairment and cerebellar dysfunction in relapsing-remitting multiple sclerosis. *Journal of the Neurological Sciences*, *347*(1-2), 246–250. http://doi.org/10.1016/j.jns.2014.10.008

Rypma, B., & Prabhakaran, V. (2009). When less is more and when more is more: The mediating roles of capacity and speed in brain-behavior efficiency. *Intelligence*, *37*(2), 207–222. http://doi.org/10.1016/j.intell.2008.12.004

Rypma, B., Berger, J. S., Prabhakaran, V., Bly, B. M., Kimberg, D. Y., Biswal, B. B., & D'Esposito, M. (2006). Neural correlates of cognitive efficiency. *NeuroImage*, *33*(3), 969–979. http://doi.org/10.1016/j.neuroimage.2006.05.065

Salthouse, T. A. (1996). The processing-speed theory of adult age differences in cognition. *Psychological Review*, *103*(3), 403–428.

Salthouse, T. A. (2000). Aging and measures of processing speed. *Biological Psychology*, *54*(1-3), 35–54.

Salthouse, T. A., Habeck, C. G., Razlighi, Q., Barulli, D., Gazes, Y., & Stern, Y. (2015). Breadth and age-dependency of relations between cortical thickness and cognition. *Neurobiology of Aging*, *36*(11), 3020–3028. http://doi.org/10.1016/j.neurobiolaging.2015.08.011

Sambataro, F., Murty, V. P., Callicott, J. H., Tan, H.-Y., Das, S., Weinberger, D. R., & Mattay, V. S. (2010). Age-related alterations in default mode network: impact on working memory performance. *Neurobiology of Aging*, *31*(5), 839–852. http://doi.org/10.1016/j.neurobiolaging.2008.05.022

Schmiedek, F., Oberauer, K., Wilhelm, O., Süß, H.-M., & Wittmann, W. W. (2007). Individual differences in components of reaction time distributions and their relations to working memory and intelligence. *Journal of Experimental Psychology: General*, *136*(3), 414–429. http://doi.org/10.1037/0096-3445.136.3.414

Schneider, W. J., & McGrew, K. S. (2012). The Cattell-Horn-Carroll model of intelligence. In *Contemporary Intellectual Assessment*.

Schretlen, D., Pearlson, G. D., Anthony, J. C., Aylward, E. H., Augustine, A. M., Davis, A., & Barta, P. (2000). Elucidating the contributions of processing speed, executive ability, and frontal lobe volume to normal age-related differences in fluid intelligence. *Journal of the International Neuropsychological Society*, *6*(1), 52–61. http://doi.org/10.1017/S1355617700611062

Schwarz, W. (2001). The ex-Wald distribution as a descriptive model of response times. *Behavior Research Methods, Instruments, & Computers*, *33*(4), 457–469.

Selya, A. S., Rose, J. S., Dierker, L. C., Hedeker, D., & Mermelstein, R. J. (2012). A Practical Guide to Calculating Cohen's f(2), a Measure of Local Effect Size, from PROC MIXED. *Frontiers in Psychology*, *3*, 111. http://doi.org/10.3389/fpsyg.2012.00111

Shine, J. M., & Shine, R. (2014). Delegation to automaticity: the driving force for cognitive evolution? *Frontiers in Neuroscience*, *8*(116), 90. http://doi.org/10.3389/fnins.2014.00090

Smith, R. L., Ager, J. W., & Williams, D. L. (1992). Suppressor Variables in Multiple Regression/Correlation. *Educational and Psychological Measurement*, *52*(1), 17–29. http://doi.org/10.1177/001316449205200102

Smith, S. M., Jenkinson, M., Woolrich, M. W., Beckmann, C. F., Behrens, T. E. J., Johansen-Berg, H., et al. (2004). Advances in functional and structural MR image analysis and implementation as FSL. *NeuroImage*, *23 Suppl 1*, S208–19. http://doi.org/10.1016/j.neuroimage.2004.07.051

Sobczak-Edmans, M., Lo, Y.-C., Hsu, Y.-C., Chen, Y.-J., Kwok, F. Y., Chuang, K.-H., et al. (2019). Cerebro-Cerebellar Pathways for Verbal Working Memory. *Frontiers in Human Neuroscience*, *12*, 1079. http://doi.org/10.3389/fnhum.2018.00530

Sokolov, A. A., Zeidman, P., Erb, M., Ryvlin, P., Friston, K. J., & Pavlova, M. A. (2018). Structural and effective brain connectivity underlying biological motion detection. *Proceedings of the National Academy of Sciences*, *115*(51), E12034–E12042. http://doi.org/10.1073/pnas.1812859115

Sridharan, D., Levitin, D. J., & Menon, V. (2008). A critical role for the right fronto-insular cortex in switching between central-executive and default-mode networks. *Proceedings of the National Academy of Sciences*, *105*(34), 12569–12574. http://doi.org/10.1073/pnas.0800005105

Stankov, L., & Roberts, R. D. (1997). Mental speed is not the “basic” process of intelligence. *Personality and Individual Differences*, *22*(1), 69–84. http://doi.org/10.1016/s0191-8869(96)00163-8

Stoodley, C. J., & Schmahmann, J. D. (2010). Evidence for topographic organization in the cerebellum of motor control versus cognitive and affective processing. *Cortex*, *46*(7), 831–844. http://doi.org/10.1016/j.cortex.2009.11.008

Takeuchi, H., Sugiura, M., Sassa, Y., Sekiguchi, A., Yomogida, Y., Taki, Y., & Kawashima, R. (2012). Neural correlates of the difference between working memory speed and simple sensorimotor speed: an fMRI study. *PLoS ONE*, *7*(1), e30579. http://doi.org/10.1371/journal.pone.0030579

Tark, K.-J., & Curtis, C. E. (2009). Persistent neural activity in the human frontal cortex when maintaining space that is off the map. *Nature Neuroscience*, *12*(11), 1463–1468. http://doi.org/10.1038/nn.2406

Tibshirani, R. (1996). Regression Shrinkage and Selection via the Lasso. *Journal of the Royal Statistical Society. Series B Methodological*, *58*(1), 267–288.

Tibshirani, R. (2011). Regression shrinkage and selection via the lasso: a retrospective. *Journal of the Royal Statistical Society: Series B (Statistical Methodology)*, *73*(3), 273–282. http://doi.org/10.1111/j.1467-9868.2011.00771.x

Turken, A., Whitfield-Gabrieli, S., Bammer, R., Baldo, J. V., Dronkers, N. F., & Gabrieli, J. D. E. (2008). Cognitive processing speed and the structure of white matter pathways: convergent evidence from normal variation and lesion studies. *NeuroImage*, *42*(2), 1032–1044. http://doi.org/10.1016/j.neuroimage.2008.03.057

Verhaeghen, P. (2011). Aging and Executive Control: Reports of a Demise Greatly Exaggerated. *Current Directions in Psychological Science*, *20*(3), 174–180. http://doi.org/10.1177/0963721411408772

Verhaeghen, P. (2013a). Lifespan Trajectories. *The Elements of Cognitive Aging* (pp. 211–247). http://doi.org/10.1093/acprof:oso/9780195368697.003.0007

Verhaeghen, P. (2013b). Toward a Sparse Ontology of Age Effects in Elementary Processes. *The Elements of Cognitive Aging* (pp. 142–168). http://doi.org/10.1093/acprof:oso/9780195368697.003.0005

Vincent, J. L., Kahn, I., Snyder, A. Z., Raichle, M. E., & Buckner, R. L. (2008). Evidence for a frontoparietal control system revealed by intrinsic functional connectivity. *Journal of Neurophysiology*, *100*(6), 3328–3342. http://doi.org/10.1152/jn.90355.2008

Vincent, J. L., Patel, G. H., Fox, M. D., Snyder, A. Z., Baker, J. T., Van Essen, D. C., et al. (2007). Intrinsic functional architecture in the anaesthetized monkey brain. *Nature*, *447*(7140), 83–86. http://doi.org/10.1038/nature05758

Wager, T. D., Sylvester, C.-Y. C., Lacey, S. C., Nee, D. E., Franklin, M., & Jonides, J. (2005). Common and unique components of response inhibition revealed by fMRI. *NeuroImage*, *27*(2), 323–340. http://doi.org/10.1016/j.neuroimage.2005.01.054

Wechsler, D. (2008). Wechsler Adult Intelligence Scale–Fourth Edition (WAIS-IV). San Antonio, TX: The Psychological Corporation.

Weissman, D. H., & Carp, J. (2013). The congruency effect in the posterior medial frontal cortex is more consistent with time on task than with response conflict. *PLoS ONE*, *8*(4), e62405. http://doi.org/10.1371/journal.pone.0062405

Weissman, D. H., Roberts, K. C., Visscher, K. M., & Woldorff, M. G. (2006). The neural bases of momentary lapses in attention. *Nature Neuroscience*, *9*(7), 971–978. http://doi.org/10.1038/nn1727

Weissman, D. H., Woldorff, M. G., Hazlett, C. J., & Mangun, G. R. (2002). Effects of practice on executive control investigated with fMRI. *Brain Research. Cognitive Brain Research*, *15*(1), 47–60. http://doi.org/10.1016/s0926-6410(02)00215-x

Wilhelm, O., & Oberauer, K. (2006). Why are reasoning ability and working memory capacity related to mental speed? An investigation of stimulus–response compatibility in choice reaction time tasks. *European Journal of Cognitive Psychology*, *18*(1), 18–50. http://doi.org/10.1080/09541440500215921

Woodward, N. D., Duffy, B., & Karbasforoushan, H. (2013). Prefrontal cortex activity during response selection predicts processing speed impairment in schizophrenia. *Journal of the International Neuropsychological Society*, *19*(7), 782–791. http://doi.org/10.1017/S1355617713000532

Wu, T. T., Chen, Y. F., Hastie, T., Sobel, E., & Lange, K. (2009). Genome-wide association analysis by lasso penalized logistic regression. *Bioinformatics*, *25*(6), 714–721. http://doi.org/10.1093/bioinformatics/btp041

Yang, Z., Ye, C., Bogovic, J. A., Carass, A., Jedynak, B. M., Ying, S. H., & Prince, J. L. (2016). Automated cerebellar lobule segmentation with application to cerebellar structural analysis in cerebellar disease. *NeuroImage*, *127*, 435–444. http://doi.org/10.1016/j.neuroimage.2015.09.032

Yeo, B. T. T., Krienen, F. M., Sepulcre, J., Sabuncu, M. R., Lashkari, D., Hollinshead, M., et al. (2011). The organization of the human cerebral cortex estimated by intrinsic functional connectivity. *Journal of Neurophysiology*, *106*(3), 1125–1165. http://doi.org/10.1152/jn.00338.2011